ADDIS ABABA UNIVERSITY

ADDIS ABABA INSTITUTE OF TECHNOLOGY

SCHOOL OF CIVIL AND ENVIRONMENTAL ENGINEERING

THE INFLUENCE OF BOND DETERIORATION ZONE ON TENSION STIFFENING OF FLEXURAL MEMBERS ON SHORT-TERM DEFLECTION

A Thesis in Structural Engineering

By Bezawit Temesgen

Oct. 2019
Addis Ababa

A Thesis

Submitted in Partial Fulfillment of the Requirements for the Degree of Master of Science

The undersigned have examined the thesis entitled 'The influence of bond deterioration zone on tension stiffening of flexural members on short-term deflection' presented by Bezawit Temesgen, a candidate for the degree of Master of Science and hereby certify that it is worthy of acceptance.

Esayas Gebreyouhannes (PhD)		
Advisor	Signature	Date
Girma Zerayohannes (PhD)		
Internal Examiner	Signature	Date
Asnake Adammu (PhD)		
External Examiner	Signature	Date
Yonas Solomon		
Chair person	Signature	Date

UNDERTAKING

I certify that research work titled "The influence of bond deterioration zone on tension stiffening of flexural members on short-term deflection" is my own work. The work has not been presented elsewhere for assessment. Where material has been used from other sources it has been properly acknowledged / referred.

Bezawit Temesgen

ABSTRACT

The bond between concrete and steel bars is of fundamental importance to deformation characteristics of cracked concrete structures. It has been studied for many years. But the results of the studies seem to be inadequate for concrete structure analysis. They are not reflected in engineering practice and codes. This affects the load caring capacity and deformational behavior of a beam. Moreover, the present design trend introduces the use of higher strength concrete and reinforcement which leads to longer spans and smaller depth of beams, for this case deformations are often the governing design criteria.

In this study, the impacts of bond degradation on tension stiffening are examined in an analytical model. A method for calculating short-term deflection is proposed by considering these impacts. Also available experimental data is assessed which confirmed the theoretical predictions.

Key words: tension stiffening, bond deterioration zone, short term deflection

ACKNOWLEDGMENTS

First of all, I would like to praise my Father God who helped me and was with me with his favor everywhere and in every step of my life. Then, my sincere gratitude goes to my advisor, Dr. Esayas G/Youhannes, for his guidance, continued support and incredible patience throughout my research. The thesis would not have been possible without his continuous encouragement and supervision. I would also like to thank Yisshak Tadesse for clearing up my confusion on his thesis. Even in his petty moment, he took his time to explain.

I would like to express my heartfelt gratitude to my friends, Tsigereda Getachew, Noah Girma, and Abenezer Negussie, for the experimental result. They were so kind and dedicated to provide every information I need. Last but certainly not least, I would like to thank my family and friends for their invaluable support.

TABLE OF CONTENTS

LIST OF TABLES

LIST OF FIGURES

1. INTRODUCTION

1.1 General Background

Typical reinforced concrete structures are designed assuming that concrete and steel bars work together in carrying loads. As long as there are no cracks in the tension zone, the interaction is based on ideal primary bond. This means that in any cross section, the strain value in a steel bar is the same as in the adjacent concrete. At such load levels the bond is based on adhesion forces. After cracking the situation is much more complicated. The strains in the steel are much greater than the ones in the concrete and slip occurs between the steel bar and the surrounding concrete, which breaks the adhesion. Due to residual bond with reinforcement, the cracked concrete between cracks carries a certain amount of tensile force normal to the cracked plane. Concrete adheres to reinforcement bars and contributes to overall stiffness of the structure.

Reinforced concrete structures designed according to present building codes as member property rather than a section. But these approaches fail to fully incorporate the tension stiffening and bond deterioration zone effect which mainly is the attribute of the intact concrete between cracked sections. Assumption of a tension-stiffening law has great influence on numerical results of load – deflection behavior of reinforced concrete members subjected to short – term loading. (Tadesse, 2015)

The primary focus of this research is to examine the effect of bond deterioration zone on tension stiffening. Due to the splitting and crushing of concrete around the bar, the bond between concrete and steel reinforcement will deteriorate and this results a deterioration zone. An analytical model is developed including these effects and results are compared with available experimental data.

1.2 Objective

The objective of this thesis is to investigate the current norms of calculating deflection and propose a free-of-shrinkage deflection calculation method. This method incorporates bond deterioration on tension-stiffening subjected to short-term loading.

1.3 Statement of the Problem

Design code (EBCS 2, 1995) is based on linear assumption for crack and deflection calculation. Even though (EC 2, 1992) and (ACI 318, 2008) include the nonlinear property of concrete they do not reveal the actual stress-strain state of cracked structures. These methods do not fully include the tension stiffening and the bond deterioration zone effect. Even though finite element method can resolve such cases the method is tedious and is not practically simple for use in designing offices.

1.4 Scope of the research

The study will only analyze short term deflection of a reinforced concrete beams subjected to flexure. Therefore the research doesn't incorporate the long term effects resulting from shrinkage and creep.

1.5 Methodology

The overall process of this research includes literature review, examination of building codes and verification of beams by experimental program. First the deflection of a beam (Tadesse, 2015) has been evaluated and compared with the proposed method. Other beams have also been evaluated by codes, proposed method and experimental results.

1.6 Organization of the Thesis

Chapter 2 provides a review of relevant literature. Much emphasis is given to cover the effect of crack in reinforced concrete and present trend of deformational models of RC members.

Chapter 3 covers the analytical study of previous work on the deflection calculation of the proposed methods by incorporates the effect of bond deterioration on tension stiffening.

Chapter 4 is devoted to the experimental Verification. Four experimental results have taken and the current trend of deflection calculation and the proposed method is assessed.

Chapter 5 offers the conclusion of the research with a recommendation for future work.

2. LITERATURE REVIEW

The proposed research builds on the recent work by (Tadesse, 2015) who develop analysis and design recommendations in determining the short term deflection of reinforced concrete beams with due consideration to the role of the concrete in the tension zone. A new method was employed where the effect of bond deterioration zone was incorporated in the analysis procedure. The following is a brief review of relevant literature.

2.1 Theoretical Background

Steel members can be considered to be homogenous so that linear strain profile can be applied and subsequently full-interaction moment – curvature approach can be used. In contrast, the behavior of reinforced members is incredibly complex. The mechanical properties of concrete depend upon not only its constituent materials: cement, aggregate, and water, but also its mixing, compaction, and curing conditions. Thus, it is not too much to say that producing homogeneous concrete is impossible. The uncertainty in material properties makes it impossible to analyze and predict the real behavior of concrete structures with accuracy.

In a reinforced concrete member, the tensile response becomes more complicated due to the bond characteristics between reinforcing bars and concrete. The stress transfer between steel and surrounding concrete is a fundamental characteristic of reinforced concrete structures. The properties of this interaction depend on several factors, such as friction, mechanical interaction and chemical adhesion. In flexural reinforced concrete structures, deformed bars depend primarily on the mechanical interlocking for bond properties, while the contribution of chemical adhesion and friction are negligently considered. For rational analysis of reinforced concrete interfaces, mechanical behaviors of interacting components across the interfaces should be properly conceptualized. When a concrete member is under tension, it has a nonlinear stress-strain relationship due to the process of cracking between cement matrix and aggregate.

2.2 Cracking in Reinforced Concrete

Cracking in a reinforced concrete structure is unavoidable due to the low tensile strength of concrete. However, concrete does not crack suddenly and completely but undergoes progressive microcracking. A clear understanding of the tensile behaviors and a reliable model representing nonlinear tensile behaviors of concrete are needed. Therefore, in assessing the deflection of reinforced concrete members, it is necessary to incorporate the effect of cracking in the calculation.

2.2.1 Crack Formation in Concrete around Ribbed Tension Bars

When assigning tension to a ribbed reinforcement bar embedded in concrete, a certain formation of cracks appears. In (Goto, 1971) the cracking behavior was examined on pure tension members. A number of tensile members, each with a single reinforcement bar encased in the concrete, were loading to fracture. After loading, Goto study the internal cracks by injecting ink into the specimen along the reinforcement bar. When all concrete material around the reinforcement was removed, it was possible to study the internal cracks by looking at the hardened ink.

Ribbed reinforcement bars have a large influence on the cracks. The ribs in the reinforcement control a big part of the bond mechanism between the reinforcement and concrete. At some level in the loading process, a slip between the reinforcement bar and the concrete will occur, and locally the ribs will subject the concrete to compression. For plain bars, the slip will happen at a much earlier load level than for ribbed bars because only adhesion holds the plain bar from slipping.

(Goto, 1971) tests showed that two different kinds of cracks form in the concrete; primary and secondary cracks. The primary cracking happen when the tensile strain of the concrete is exceeded and these cracks form perpendicular to the loading direction. The secondary cracks are developed because of the difference in elongation in concrete and reinforcement. Because the strain of the reinforcement is larger than the concrete’s the ribs will locally subject the concrete to compression, which causes a crack to form at each rib. The first of the secondary cracks will develop around the primary cracks because the difference in strains is largest here.

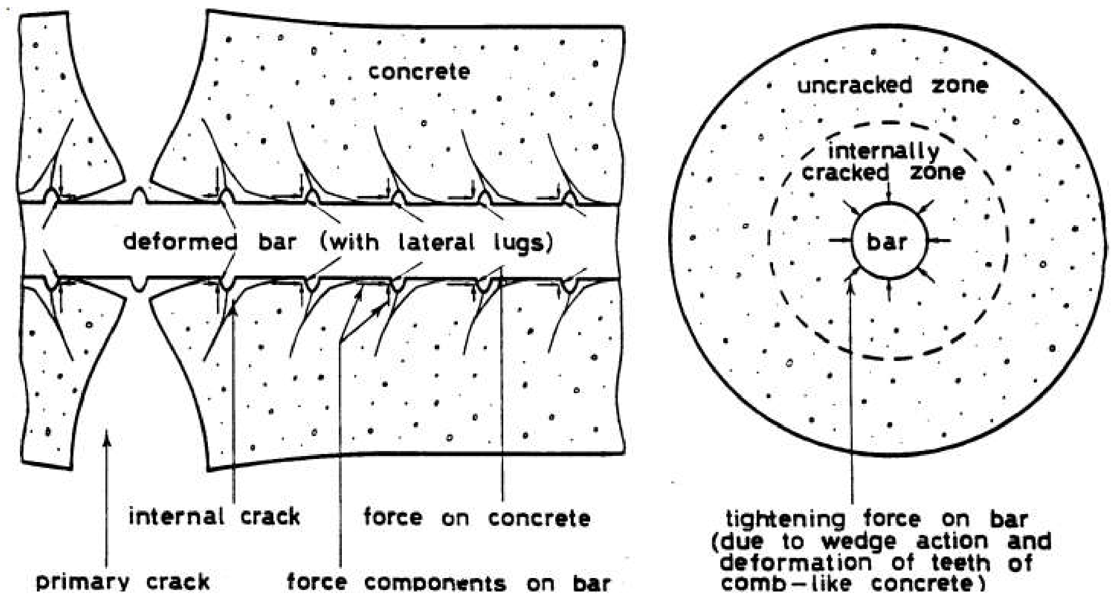

Figure 2-1: Cracking of Reinforced Concrete (Goto, 1971)

Splitting cracks are another form of secondary cracks that form parallel to the reinforcement bar. These often form at a very high stress level or when the reinforcement diameter is very large compared to the concrete cover (Abrishami 1996).

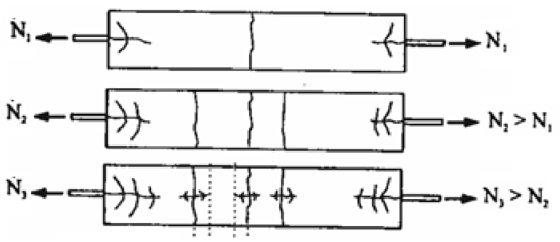

Figure 2-2: Splitting and transverse crack propagation in tests specimens from Abrishami 1996.

The behavior exhibited by a cracked reinforced concrete beam under flexure is a complex process that entails a wide range of effects, such as, different strength and deformation properties of steel and concrete, cracks that will inevitably occur, tension-softening and tension-stiffening, bond slip between reinforcement and concrete, etc.

2.2.2 Steel-Concrete Bond

The utility of reinforced concrete as a structural material is derived from the combination of concrete that is strong and relatively durable in compression with reinforcing steel that is strong and ductile in tension. Maintaining composite action requires transfer of load between the concrete and steel. This load transfer is referred to as bond and is idealized as a continuous stress field that develops in the vicinity of the steel-concrete interface.

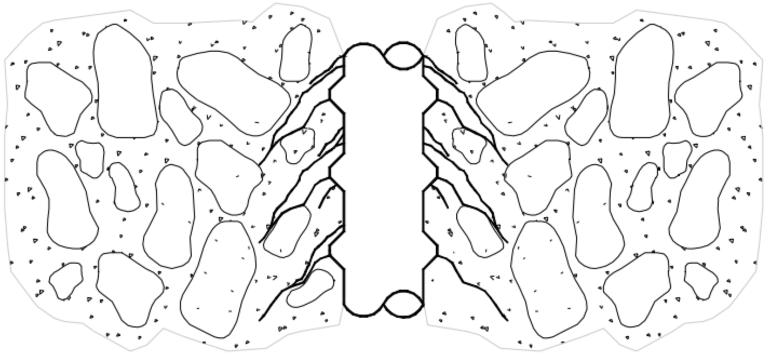

Figure 2-3: Steel-concrete bond (Maekawa, Pimanmas, & Okamura, 2004)

The bond strength of reinforced concrete is composed of chemical adhesion between concrete and reinforcing bars, the friction resistance, and mechanical interaction between steel and concrete (Lutz and Gergely 1976). Chemical adhesion mechanism is aroused firstly and prevents slip after loading. The hydration products (C-S-H gel) of cement in the concrete adheres to the surface of the steel reinforcement. This resistance is very small in comparison to the mechanical gripping resistance (Maekawa, Pimanmas, & Okamura, 2004). Slip will occur after adhesion is destroyed. Then, the other two kinds of bonding mechanisms, the friction resistance, and mechanical interlocking resistance, start to work (Chinn et al. 1955, Eligehausen et al. 1982). The steel bar is elongated more significantly as the load increases. Because of this effect, the cross section will decrease. At this moment, friction becomes negligible and mechanical resistance becomes the primary mechanism for transferring force. Cracks start to form adjacent to the rebar of steel as shown in Figure 2-3.

2.2.3 Tension Softening

The tension softening characteristics of concrete, along with its fracture energy, is an important parameter in determining the fracture property of the concrete. The fracture property of a concrete structure can be quantitatively analyzed only when both the tension softening characteristic and fracture energy have been clarified.

Further, the tension softening characteristic provides information important in evaluating the fracture property of various types of concrete, especially for their strength evaluation (Maekawa K. & Qureshi J., 1996).

In reality, the bond stress at the crack surface does not suddenly drop to zero. There is some residual stress to resist against the crack extension transferred by the interlocking of the two faces. This phenomenon is known as tension softening of plain concrete. The effect of this softening in reinforced concrete members with ordinary reinforcement ratios is insignificant compared to the force carried by bond stress transfer. Yet, (Salem & Maekawa, 1999) observed the importance of considering tension softening at cracked sections arises in lightly reinforced concrete, as its contribution becomes higher compared to the contribution of bond stress transfer.

Tension softening (Qureshi & Maekawa , 1996) is expressed as a relationship between the residual tensile stress and the crack width, which is the main parameter of tension softening. The surface crack width can be considered being compatible with the reinforcement slip at the crack. The average crack width is

$$w = C(2S_{max}), S_{max} = S/_{x=L_c/2} \qquad \text{Eq. 2.1}$$

Where C=1/1.3.

The tension softening model adopted in the analysis is defined as,

$$\sigma_{br} = f_t \left[1 + 0.5\left(\frac{f_t}{G_f}\right) w\right]^{-3} \qquad \text{Eq. 2.2}$$

Where, σ_{br} is the bridging stress across the crack, f_t is the tensile strength, w is the crack width and G_f is the fracture energy.

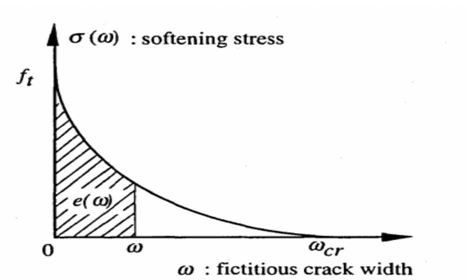

Figure 2-4: Tension Softening Curve (Maekawa K. & Qureshi J., 1996)

$$G_F = e(\omega_{cr}) = \int_0^{\omega} \sigma(\omega)\, d\omega \qquad \text{Eq. 2.3}$$

Where, G_F is the fracture energy of concrete ranges from 0.1 to 0.15 N/mm for plain concrete.

2.2.4 Tension Stiffening

When a reinforced concrete member is subjected to a tensile force, the tensile force is distributed to the bars and concrete according to the ratio of their modulus of elasticity. The first crack occurs when the stress of concrete overcomes the tensile strength, and the load carried at the cracked section by the steel bars is gradually transferred to the concrete at each side of the crack by bond between steel and concrete. As the applied load increases, additional cracks form at discrete intervals along the member. Although the total load is entirely carried by the bars at cracks, concrete between cracks takes a part of the force due to existence of bond. The average tensile stiffness becomes intermediate between that of the uncracked and fully cracked reinforced concrete, and this is called as "Tension stiffening effect." (Goto, 1971)

The tension stiffness of cracked concrete has an influence on the deformation and crack width of reinforced concrete members (Goto, 1971). Furthermore, the crack width affects the shear transfer and finally, the shear transfer affects the ultimate strength of reinforced concrete members subjected to forces. (Tadesse, 2015) emphasize the necessity of the consideration of tension stiffening effect for accurate prediction of deflection.

2.2.5 Bond Deterioration Zone

When reinforcing bar is tensioned against concrete, splitting conical cracks appear because the ribs of the reinforcing bar press against concrete causing conical diagonal compressive struts. (Qureshi & Maekawa , 1996). Splitting cracks are shown in Figure 2-1 and Figure 2-5.

Figure 2-5: Splitting conical cracks

Indirection perpendicular to these compressive struts tensile stresses are generated causing these splitting conical cracks. In the area of crack planes, these compressive struts have no concrete to support because of the penetration of conical cracks reaching to the crack planes. So that, concrete spalling takes place causing bond deterioration (Maekawa K. & Qureshi J., 1996). Thus modeling bonds close to cracks plays an important role in the calculation of deflection.

2.3 Experimental and Analytical Studies on Tension stiffening and bond deterioration zone.

2.3.1 Experimental Studies on Tension stiffening and bond deterioration zone.

Several previous studies were carried out separately to develop constitutive models for both steel and concrete components, but most of them were verified under simplified and idealized loading conditions. For instance, (Shima H. , Chou L. , & Okamura, H. , 1987) reinforcement modeling was treated by considering separately the two actions of the axial pullout and transverse shear and then superimposing these behaviors.

Since the bond-slip-strain model proposed by (Shima H. , Chou L. , & Okamura, H. , 1987) was formulated under pure tensile conditions, the presence of transverse displacement to the axis of bars is not taken into account for computing axial stress - pullout relation. (Mishima, Yamada, & Maekawa, 1992) examined the ability of the these suggestion. Through series of experimental verification, it was clarified that reinforced concrete normal cracks, which are introduced by tension stress in concrete and reinforced by deformed bars of reinforcement ratio not greater than 2%, can be successfully dealt with by the simple superposition law of stress transfer of concrete crack, and the bond-slip model of a single reinforcing bar.

(Maekawa K. & Qureshi J., 1996) deals with the behaviors of embedded deformed reinforcing bars under a coupled opening interface and transverse shear displacement that can be supplied for computational models. The research shows that the simple superposition law brings overestimated shear capacity of reinforced concrete crack planes and higher shear stiffness than reality when the higher reinforcement ratio is provided.

From experiments in this study (Maekawa K. & Qureshi J., 1996), it can be considered that a primary source of the reduced shear capacity might originate from the lowered confinement efficiency against crack opening of embedded bars due to reduced axial capacity of steel mobilized by shear slip along the crack. It will accelerate the reduction of pullout stiffness and strength in turn, finally determining the ultimate shear capacity.

Recent developments as well (Maekawa, Pimanmas, & Okamura, 2004) suggest that even if pull-out slip test along the axis of the bars only is easy to compute but it didn't give a reliable result. Reinforced concrete must be treated with coupled pull-out and transverse shear displacement in order to obtain accurate behavior.

In reference (Maekawa K. & Qureshi J., 1996), it has been reported that the non-uniformity in the distribution of mean strains close to the crack plane, with some extreme fibers in the reinforcement reaching plastic strains at certain sections, while the mean strain at the interface and at other points away from the interface was found to be elastic even up to ultimate loads.

2.3.2 Analytical Studies on Tension stiffening and bond deterioration zone.

Modeling of reinforcement under uniaxial pullout has been proposed by several researchers, who have established microscopic and macroscopic bond models. (Shima H. , Chou L. , & Okamura, H. , 1987) formulated a constitutive model for bond stress, strain and axial slip considering both microscopic and macroscopic aspects of the bond. This model is taken as a framework for modification to propose the enhanced model for the embedded bar under generic displacement paths.

(Shima H. , Chou L. , & Okamura, H. , 1987) assumed that the reinforcing bar stress has a full cosine profile, and based on this distribution they got the average stress-average strain relationship of reinforcing bars. Their choice of a cosine stress distribution was based on the fact that cosine function is a symmetric one and its derivative is zero at both the cracked section and the center of the segment. This agrees well with the fact that the bond stresses at the cracks and at the midway between two successive cracks are zero.

$$f_{so} = f_s + a_s \, Cos\frac{2\pi x}{L}$$

Eq. 2.4

Where:- a_s is the amplitude of the cosine curve.

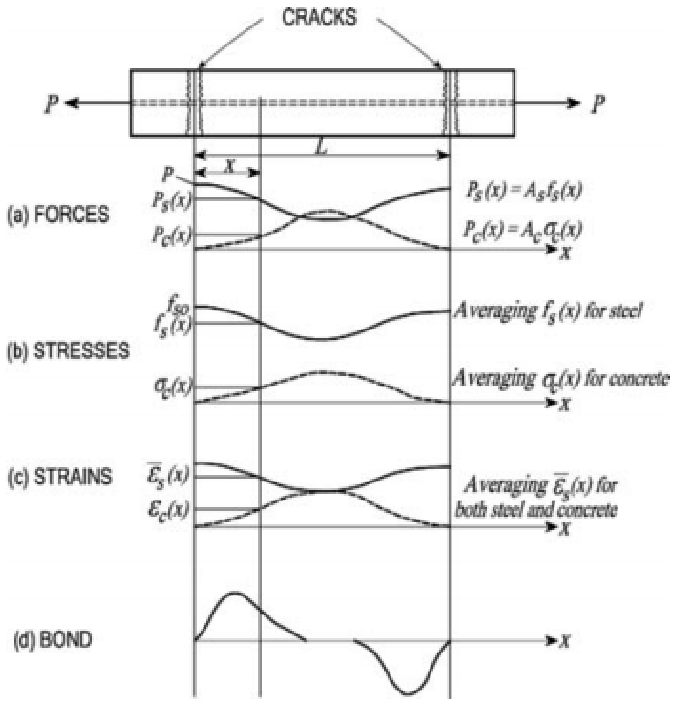

Figure 2-6: Stresses and strains between two cracks (Hsu, Thomas, & Mo, 2010)

(Belarbi & Hsu, 1991) assumed another stress profile, summing up the cosine function of Shima and two other sinusoidal functions. The aim of this modification was to simulate the fact that the bond stress between reinforcing bars and concrete deteriorates after crack initiates and the reinforcing bar stress becomes uniform around the cracks.

$$f_{so} = f_s + a_s \, Cos\frac{2\pi x}{L} + b_s \left(Sin\frac{3\pi x}{L} + 0.6 Sin\frac{5\pi x}{L} - 0.1358 \right)$$

Eq. 2.5

Where:- the added term b_s, 0.6 and 0.1358 were chosen to satisfy the boundary conditions at the cracks and at the midpoint between the cracks

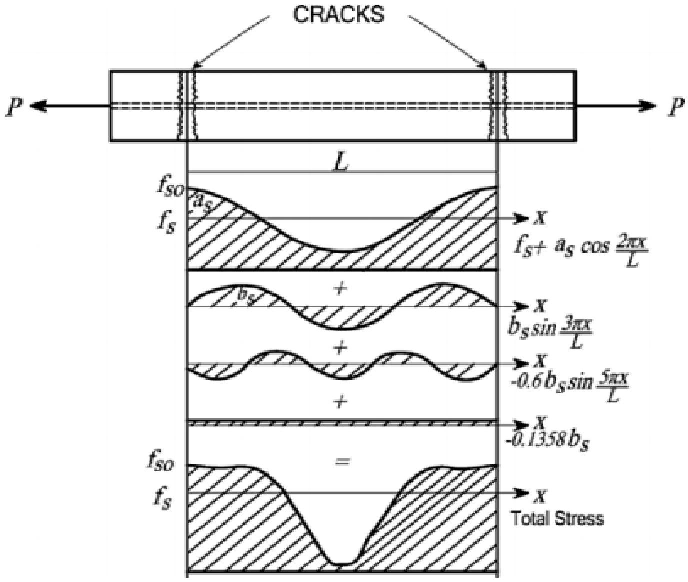

Figure 2-7: Belarbi's stress distribution along a reinforcing bar after cracking (Belarbi & Hsu, 1991)

In lightly reinforced concrete, the importance of considering tension stiffening and tension softening in cracked sections arises as its contribution becomes higher compared to the contribution of bond stress transfer (Salem & Maekawa, 1999). For middle and highly reinforced concrete both Shima and Belarbi are acceptable, where the spacing of cracks is relatively small. However, for lightly reinforced concrete, the crack spacing is larger and tends to be localized like plain concrete.

In Shima and Belarbi's modeling, bond deterioration is indirectly taken into account and the absolute value of crack spacing is not necessarily incorporated, by assuming similarity of stress profile between cracks. The models are very accurate under the idealized condition where no bond deterioration zone is formed in the analysis domain and sufficiently long embedment length develops, this model cannot be directly applied where the bond deterioration zone is always created, mainly in lightly reinforced concrete.

The original model of Shima (Shima H. , Chou L. , & Okamura, H. , 1987) is empirical and does not take into consideration the amount of reinforcement. Furthermore, it was derived from specimens that were free of splitting cracks and concrete spalling. It is thus not directly applicable to express the bond stress in the deterioration zone (Salem & Maekawa, 1999). As a matter of fact, the amount of reinforcement has a considerable effect on the tension stiffening of lightly reinforced members (Belarbi & Hsu, 1991).

(Qureshi & Maekawa , 1996) re-formulate the average-based tension model of cracked concrete and embedded reinforcement, using a direct theoretical derivation from microscopic mechanics. In this way, the deterioration near the cracking plane and the fracture process at a crack section is accurately considered. In computing the critical ductility, when the steel ruptures inside the concrete, a microscopic approach is indispensable since the rupture criterion is set for the local behavior of the steel.

Furthermore, for low reinforcement cases in which the simplified stress profile cannot be applied direct theoretical derivation is the precise approach. The analysis aims at obtaining a versatile smeared tension model for reinforcing bars and concrete in both heavily and lightly reinforced concrete. At the same time, the average crack spacing and the average ultimate stress can be computed.

(Qureshi & Maekawa , 1996) and (Soltani, An, & Maekawa, 2003) assumed that bond stress linearly decreases to zero at a distance 5d and that drops suddenly to zero at a distance 5d from the crack surface (Figure 2-8).

$$\tau_b(x) = \tau_{b,max} - \frac{\tau_{b,max}}{L_b}\{x - (L_e - L_b\} \qquad (L_e - L_b \leq x \leq L_e - L_b/2)$$
$$\tau_b(x) = 0 \qquad (L_e - L_b/2 \leq x \leq L_e) \qquad \text{Eq. 2.6}$$

where $\tau_{b,max}$ is the maximum bond stress attained at the origin of L_b. L_e is the bar embedded length. The bond stress profile along the embedded length, including the newly introduced profile for the concept of a bond deterioration zone, is shown in Figure 2-8.

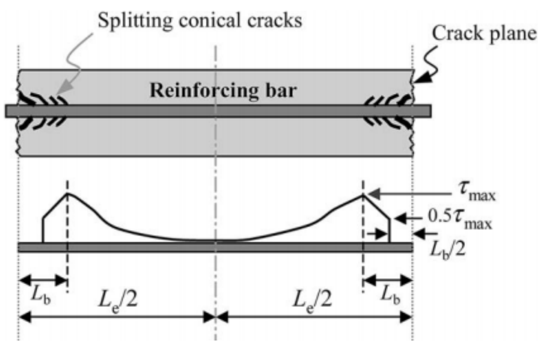

Figure 2-8: Bond deterioration beside the crack surface (Soltani, An, & Maekawa, 2003)

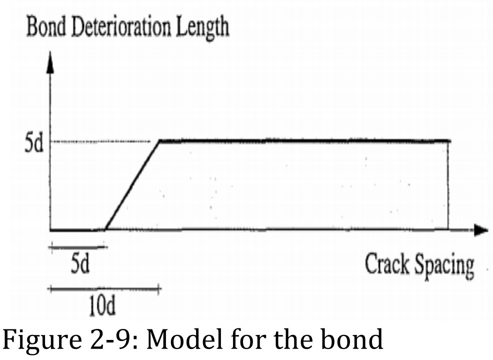

Figure 2-9: Model for the bond deterioration zone (Salem & Maekawa, 1999)

An important consideration, however, is that when the spacing of the crack falls below 10d, the length of the bond deterioration cannot logically equal 5d as the conical splitting cracks cannot meet physically. Also, when the spacing of crack drops below 5d, there can be no concrete spalling. Consequently, it was assumed that the bond deterioration length is equal to zero when the crack spacing is less than 5d, and it changes linearly from zero to 5d when the crack spacing changes from 5d to 10d as shown in Figure 2-9. However, this condition rarely happens and only in situations where the reinforcement ratio is very high and the tension strength is so small.

2.4 Short-term Deformation of Flexural RC Beams

The bending deformations, deflections and rotations, of a member are, in general, calculated from the basic moment–curvature relationships of the sections along the member, as shown in Figure 2-11. In the simple case of a homogeneous elastic member, however, the curvature ϕ is proportional to the moment *M* and the proportionality constant is the bending rigidity EI.

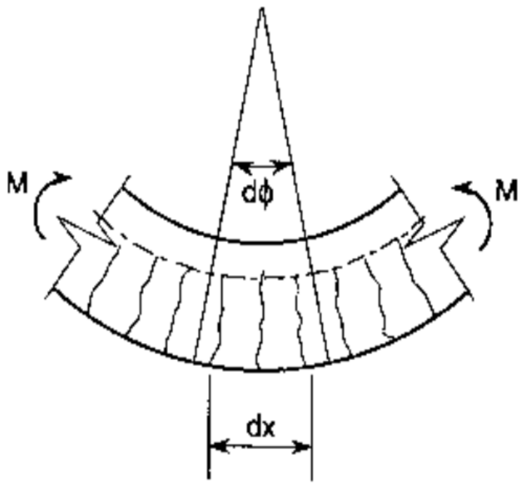

Figure 2-10: Curvature of Beam Under Uniform Bending (Hsu, Thomas, & Mo, 2010)

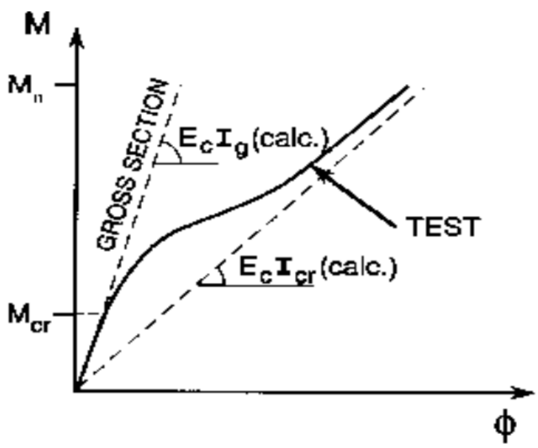

Figure 2-11: Moment-Curvature Relationship (M-ϕ) Curve (Hsu, Thomas, & Mo, 2010)

Since the curvature ϕ is defined as the bending rotation per unit length ($d\phi/d_x$), the differential bending rotation d is expressed for a differential length d_x as

$$d\emptyset = \frac{M}{EI}dx$$ Eq. 2.7

The deflections and rotations of a member can be calculated from Equation 2.7 by integration. The difficulty of applying Equation 2.7 to reinforced concrete beams with both cracked and un-cracked sections is the EI bending rigidity estimation. To overcome this difficulty it is introduced an effective bending rigidity E_cI_e, which can be used in connection with Equation 2.7 to calculate the deflections.

2.4.1 Effective Bending Rigidities

The effective bending rigidity E_cI_e is the product of two quantities E_c and I_e. E_c is the modulus of elasticity of concrete defined by:

$$E_c = g\sqrt{f'_c\,[Mpa]}$$ Eq. 2.8

Where: f'_c is the characteristic compressive strength of concrete.

I_e is the effective moment of inertia. A uniform moment M acting on a length of beam is expected to create a curvature $\phi = d\phi/dx$, as shown in Figure 2-10. The moment–curvature relationship (M–ϕ curve) is plotted in Figure 2-11. Up to the cracking moment M_{cr}, the curve follows approximately a slope calculated from the bending rigidity E_cI_g of the gross un-cracked section. After cracking, however, the curve changes direction drastically. When the nominal moment M_n is reached, the slope approaches the bending rigidity E_cI_{cr}, calculated by the cracked section.

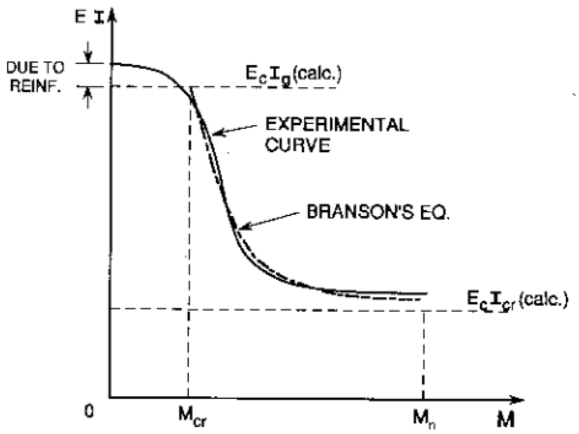

Figure 2-12: Bending Rigidity EI as a function of Moment M (Hsu, Thomas, & Mo, 2010)

The trend described above can be clearly illustrated by plotting the bending rigidity EI against the moment M in Figure 2-12. Below the cracking moment M_{cr}, the experimental curve is roughly horizontal at the level of the calculated E_cI_g. After cracking, however, the curve drops drastically. When the nominal moment M_n is approached, the curve becomes asymptotic to the horizontal line of the calculated E_cI_{cr}. A theoretical equation to express the moment of inertia, therefore, must vary from I_g at cracking to I_{cr} at ultimate.

The trend of the experimental curve, Figure 2-12, can be closely approximated by a theoretical curve

$$I = \left(\frac{M_{cr}}{M}\right)^m I_g + \left[1 - \left(\frac{M_{cr}}{M}\right)^m\right] I_{cr} \leq I_g \qquad \text{Eq. 2.9}$$

Equation 2.9 satisfies the two limiting cases. First, $I = I_g$ when $M_{cr}/M = 1$. Second, $I = I_{cr}$ when M_{cr}/M approaches zero. The moment of inertia I obviously has a value between I_g and I_{cr}. The power of m for (M_{cr}/M) in Equation 2.9 was selected to best fit the experimental curve. In design practice, the effective bending rigidity is calculated from formulas available in design codes.

2.4.1.1 Overview of ACI Design Code (ACI 318)

For beam with both cracked and uncracked regions, a rigorous calculation of the deflection using numerical integration would be very tedious. For practical purposes, an effective moment of inertia I_e was proposed by Branson (1977) and adopted by the ACI Code, Section 9.5.2.3 (ACI Commitee 318, 2014):

$$I = \left(\frac{M_{cr}}{M}\right)^3 I_g + \left[1 - \left(\frac{M_{cr}}{M}\right)^3\right] I_{cr} \leq I_g \qquad \text{Eq. 2.10}$$

where M_a is the maximum moment at mid span, and the cracking moment is

$$M_{cr} = \frac{f_r I_g}{y_t} \qquad \text{Eq. 2.11}$$

In Equation 2.11 y_t is the distance from the centroidal axis of gross section to the extreme fiber in tension. f_r is the modulus of rupture defined for normal-weight concrete

$$f_r = 0.63\sqrt{f_c}\ [Mpa] \qquad \text{Eq. 2.12}$$

2.4.1.2 Overview of European Codes (Euro code 2)

In the current European Code (European Standard, 1992), the mean curvature is calculated in cracked reinforced concrete members by interpolating between the curvatures in idealized uncracked and fully cracked sections as shown in equation 2.13

$$\alpha = \zeta \emptyset_{II} + (1 - \zeta)\emptyset_{I}$$

Where $\zeta = 1 - \beta\left({}^{\sigma_{cr}}/_{\sigma}\right)^{2}$ Eq. 2.13

$\emptyset_I$ and $\emptyset_{II}$ are the curvature in idealized uncracked and fully cracked sections respectively including shrinkage and M_{cr} is the cracking moment. The coefficient β accounts for the loss of tension stiffening with time owing to additional internal- and micro-cracking under sustained load. Euro code 2 states that β should be taken as 1 for short-term loading and 0.5 for long-term loading but does not define the variation in β with time. Note that ratio σ_{cr}/σ_s may be replaced by M_{cr}/M for flexure or N_{cr}/N for pure tension, where M_{cr} is the cracking moment and N_{cr} is the cracking force.

(Tadesse, 2015) assess short-term deflection of a simply supported span beam of 7.0 m, shown in

Figure 2-13. The beam is with concrete strength class of C25/30 and steel B435B. It is loaded with a continuous load of 23.25kN/m. In this thesis, deflection is calculated by design codes (EN 2 and ACI 318) based on different assumptions. It is concluded from this study that the codes lead to deflection overestimation. But the analysis did not consider the bond deterioration impact due to the splitting and crushing of concrete around the bar next to the crack surface. The author will include the effects of bond deterioration in the current thesis. Summary of deflection calculation by design codes is shown in Table 2-1 .

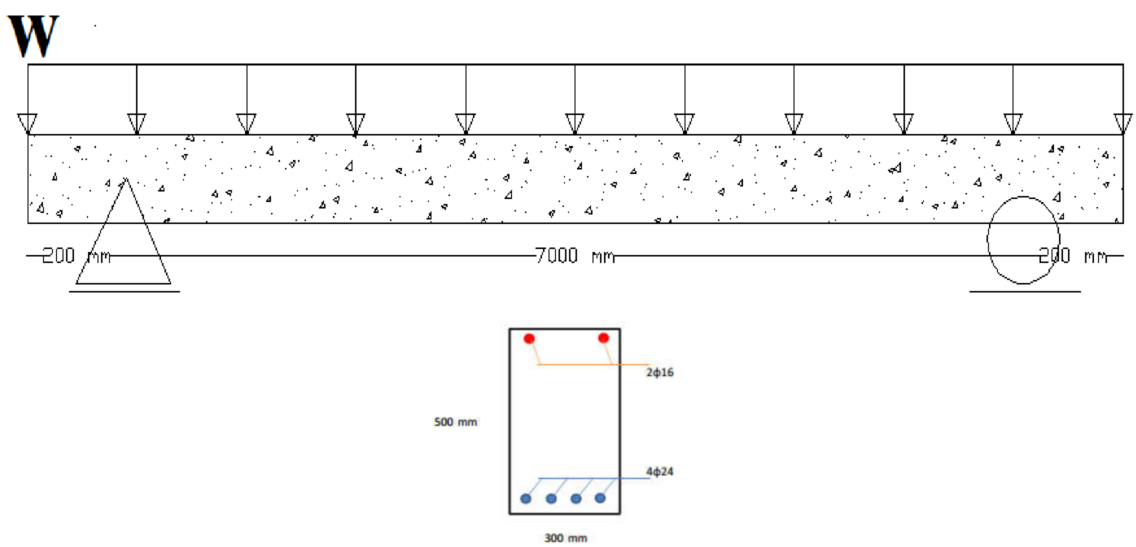

Figure 2-13: Geometry of the beam (Tadesse, 2015)

Table 2-1: Summary of the deflection calculation. (Tadesse, 2015)

x	δ ACI [mm]	δ ACI with EC2 material property [mm]	δ ACI with Bischoff's Method [mm]	δ EC2 [mm]
0.0	0.000	0.000	0.000	0.000
0.7	-2.364	-3.045	-2.731	-4.535
1.4	-7.976	-8.586	-8.722	-8.667
2.1	-12.061	-12.494	-12.887	-11.962
2.8	-14.523	-14.878	-15.452	-14.071
3.5	-15.351	-15.685	-16.322	-14.795
4.2	-14.523	-14.878	-15.452	-14.071
4.9	-12.061	-12.494	-12.887	-11.962
5.6	-7.976	-8.586	-8.722	-8.667
6.3	-2.364	-3.045	-2.731	-4.535
7.0	0.000	0.000	0.000	0.000

3. BENDING DEFLECTIONS OF REINFORCED CONCRETE BEAM

3.1 Smeared Stress–Strain Curve

The tensile load–average strain and average stress–average strain relations of bar and concrete are shown in Figure 3-1. By means of stress transfer through bonding between reinforcement and concrete, the concrete between cracks continues to carry tensile forces even after cracks occur. As a result, a RC element's tensile stiffness is higher than a single bare bar. (Goto, 1971)

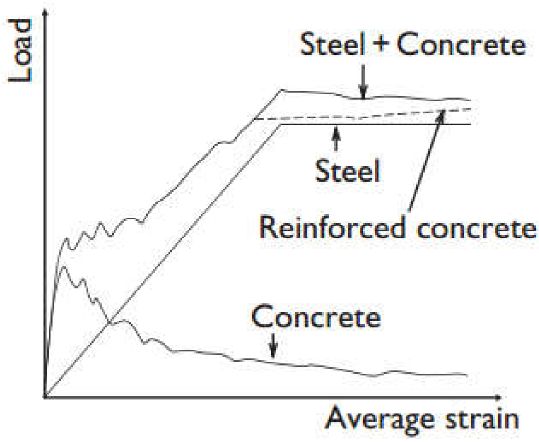

Figure 3-1: Superimposing stress of concrete and steel stresses. (Goto, 1971)

Figure 3-1 shows that the concrete between cracks carries tensile fore even in the post cracking range. As a result, the tensile stiffness of a reinforced concrete is higher than that of a bare bar. It also reveals that concrete can carry the tensile load even after the bar has yielding. Furthermore, there is no tendency of sudden reduction of tension effect in the post-yield range. This results in higher post yielding stiffness of the reinforced concrete element than that of a bare bar.

The relationship between the steel stress at cracked sections and the average stress of the bar and concrete is expressed as

$$\sigma_{cr} = \bar{\sigma}_s + \frac{\bar{\sigma}_c}{\rho} \quad \text{Eq. 3.1}$$

where σ_{cr} is steel stress at a cracked section, σ_s is average steel stress, σ_c is average concrete stress and ρ is the reinforcement ratio (= A_s/A_c).

Figure 3-2 illustrates Eq. 3.1 and the steel stress distribution between cracks schematically. Note that the distribution of steel stress was not uniform, but at the location of cracks was the highest. When the bar stress reached yield strength at the cracked sections, stresses elsewhere were still lower than yield strength. As a result, the average yielding stress of an embedded bar was lower than that of bare bar. Obviously, the average stress–strain relation of bar in RC was different from that of bare bar. Hence, the bare bar stress–strain relation should not be used in conjunction with average stress–strain of concrete for the evaluation of the tensile stiffness effects because this can lead to a mistakenly greater yield point than actually occurs. It can be seen from Eq. 3.1 and Figure 3-2 that the lower the reinforcement ratio and the yield stress of bare bar, and/or the higher the concrete strength, the lower the average yield point of the bar in an RC element.

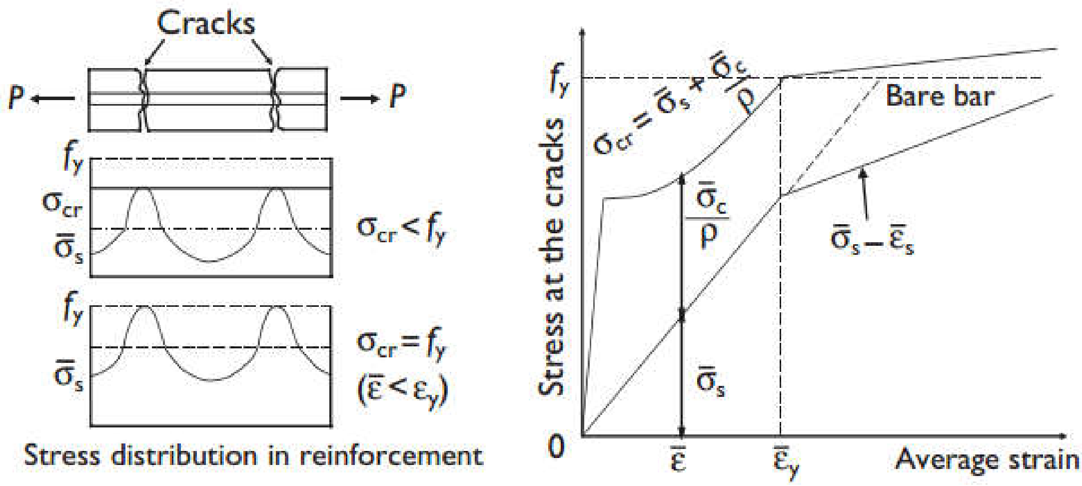

Figure 3-2: Average stress and average strain of a steel bar when yielding starts. (Hsu, Thomas, & Mo, 2010)

3.2 Constitutive Laws

3.2.1 Concrete under Tension

(Hsu, Thomas, & Mo, 2010) states a typical concrete stress-strain curve consisting of two distinct branches. Before cracked, the stress-strain relationship is essentially linear. However, after cracking, a drastic drop in force occurs and the curve's downward branch becomes concave.

$$\sigma_c = E_c \varepsilon_{cs} \qquad \varepsilon_s \leq \varepsilon_{cr} \qquad \text{Eq. 3. 2}$$

$$\sigma_c = f_{cr} \left(\frac{\varepsilon_{cr}}{\varepsilon_{cs}}\right)^{0.4} \qquad \varepsilon_s > \varepsilon_{cr} \qquad \text{Eq. 3. 3}$$

Where f_{cr} is cracking stress of concrete, taken as $0.31\sqrt{f'_c(Mpa)}$, ε_{cr} cracking strain of concrete, taken as 0.00008 mm/mm and E_c is modulus of elasticity of concrete taken as $E_c = 3875\sqrt{f'_c(Mpa)}$ and ε_{cs} strain of concrete.

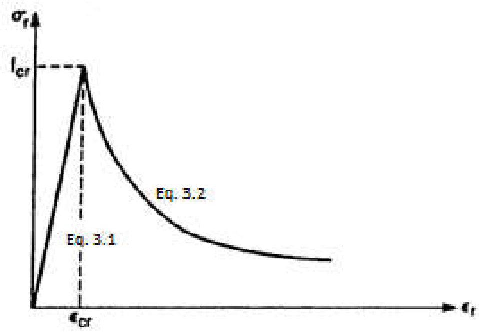

Figure 3-3: Tensile stress-strain curves of concrete (Hsu, Thomas, & Mo, 2010)

3.2.2 Steel Reinforcement

Two different idealizations, shown in

Figure 3-4, are commonly used depending on the desired level of accuracy. The first idealization neglects the strength increase due to strain hardening and the reinforcing steel is modeled as a linear elastic, perfectly plastic material, as shown in

Figure 3-4. This assumption underlies the design equations of the European code. If the strain at the onset of strain hardening is much larger than the yield strain, this approximation yields very satisfactory results.

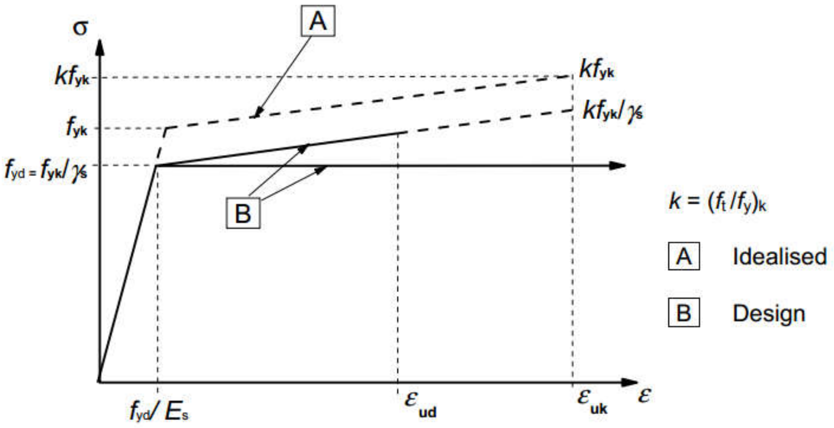

Figure 3-4: Stress-strain characteristics of reinforcement in uniaxial tension (European Standard, 1992)

3.3 Modeling the post cracking stress vs. strain relationship

The average tensile stress–strain relations of cracked concrete and embedded reinforcement can be established if their stress and strain profiles are known along the member axis. These stress and strain profiles will be analytically computed by solving simultaneously the bond-governing differential equations. These are

- **Force equilibrium**:- Static equilibrium for each part is first expressed in a differential equation which is then transformed into the finite difference form as

$$\frac{d\sigma}{dx} = \frac{\pi d}{A_s}\tau \quad \rightarrow \quad \frac{\Delta\sigma}{\Delta x} = \frac{\pi d}{A_s}\bar{\tau} \ (in\ computation) \qquad \text{Eq. 3. 4}$$

Where, dσ/dx is axial stress gradient along the axis of reinforcing bar, As, d are cross sectional area and diameter of reinforcing bar, and τ is average bond stress.

- **Deformational Compatibility: -** The slip is computed by integrating the strain over the length of the bar, starting from midway between adjacent cracks as shown in **Figure 3-5**, assuming zero slip at the midpoint between cracks.

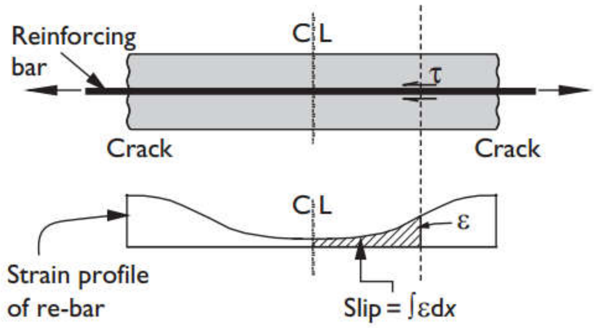

Figure 3-5: slip in bond–slip–strain model (Salem & Maekawa, 1999)

- **Bare bar stress–strain model:-** the stress vs strain diagram of a bare reinforcing bar is shown in
- Figure 3-4. Euro code 2 section 3.2.7 is used to plot the curve.
- **Bond–slip–strain model plus a bond deterioration model: -** Shima et al. proposed a universal bond stress axial slip-steel strain model for RC.

$$\tau(\varepsilon, s) = \tau_o(s)g(\varepsilon) \quad \text{Eq. 3. 5}$$

Where $\tau(\varepsilon,s)$ is local bond stress and $\tau_o(s)$ is intrinsic bond stress when strain is zero denoted by,

$$\tau_o(s) = f'_c k[ln(1 + 5s)]^c \quad \text{Eq. 3. 6}$$

$$g(\varepsilon) = \frac{1}{1 + 10^5\varepsilon} \quad \text{Eq. 3. 7}$$

Where, fc' is compressive strength of concrete, k is constant=0.3, c is constant = 3, s is non dimensional slip= 1000S/d, S is slip and d and ε are diameter and strain of the bar.

The bond model in the bond-deterioration zone is as discussed in Equation 2.7.

The overall scheme of computation is summarized in Figure 3-6. First, the spacing of the crack is equal to the total length of the target control. Load increases gradually and local stresses of both concrete and steel are computed. When the maximum local concrete stress exceeds the tensile strength of the concrete, a new crack is introduced in the middle of the specimen. The calculations are carried out again with crack spacing equal to half the initial length. In fact, the new crack spacing is the average crack spacing, since the actual location of the crack is not necessarily in the middle of the specimen. The location of the crack depends on the distribution of local tensile strength along the length of the specimen. The tensile force along the length of the specimen is not uniform due to the non-uniformity of the concrete. For simplicity, the average crack spacing is assumed. Again, the load is gradually increased and local concrete stress is checked.

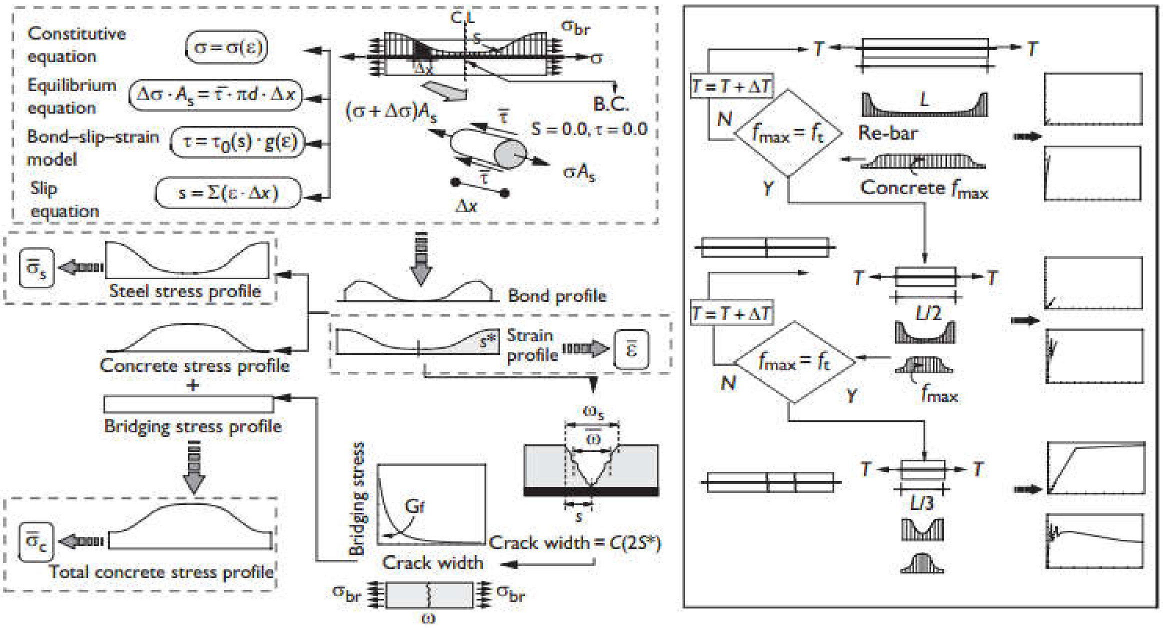

Figure 3-6: Scheme of solving bond governing equations with finite discretization (Salem & Maekawa, 1999)

To compute stress profiles, finite discretization of the reinforcing bar between two successive cracks is performed, as shown in Figure 3-6. Using a finite difference algorithm, the strain and stress profiles of the bar are obtained. The average stress and strain of steel can then be calculated as

$$\bar{\varepsilon} = \frac{2}{L_c}\int_0^{L_c/2} \varepsilon(x)dx \cong \frac{2}{L_c}\sum_0^{L_c/2} \varepsilon(x)\Delta x \qquad \text{Eq. 3. 8}$$

$$\bar{\sigma_s} = \frac{2}{L_c}\int_0^{L_c/2} \sigma_s(x)dx \cong \frac{2}{L_c}\sum_0^{L_c/2} \sigma_s(x)\Delta x \qquad \text{Eq. 3. 9}$$

Once the stress profile for the reinforcement is obtained, the stress profile for the concrete is computed by subtracting the reinforcement force profile from the reinforcing bar force at cracking and dividing the remainder by the concrete cross-sectional area. Adding the bridging stress given in Eq. 2.2, the average stress of concrete can be calculated as

$$\bar{\sigma_s} = \sigma_{br} + \frac{2}{L_c}\int_0^{L_c/2} \sigma_s(x)dx \cong \sigma_{br} + \frac{2}{L_c}\sum_0^{L_c/2} \sigma_s(x)\Delta x \qquad \text{Eq. 3. 10}$$

The finite discretization of mild steel between two successive cracks, embedded in concrete, is not an easy task and would require integration and average. In order to overcome this, the FORTRAN program is prepared for the purpose of this thesis as presented out in Appendix A and B. The flow chart of the program is shown in Figure 3-7.

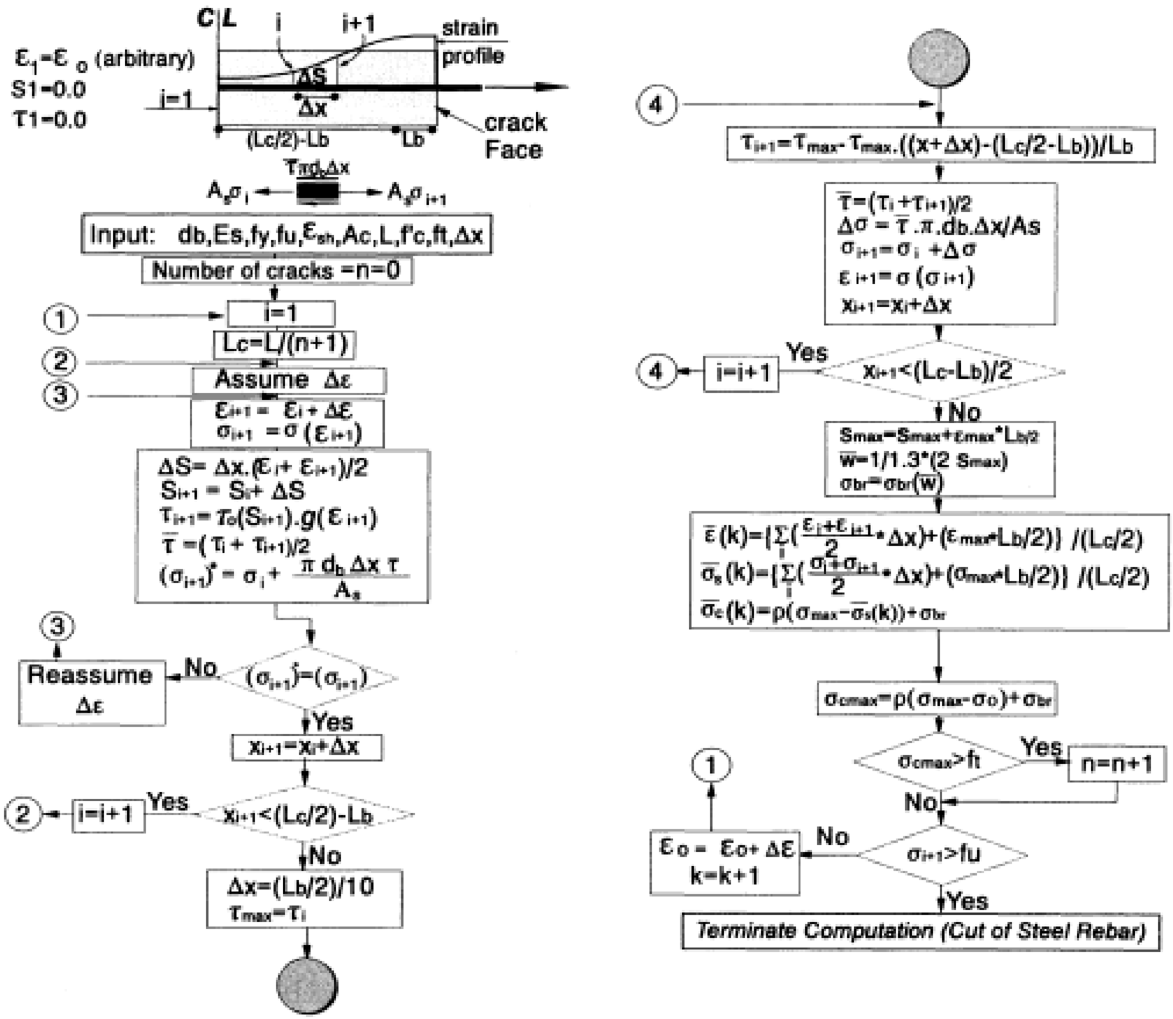

Figure 3-7: Flow chart of solving bond governing equations with finite discretization (Qureshi & Maekawa , 1996)

In order to show the effect of the bond deterioration zone on tension stiffening, the stress strain curve of 1200 mm diameter 20 B500B reinforcement bar embedded in

100 x 100 mm C25/30 concrete is used. The beam's stress vs strain curve is plotted with and without the bond deterioration zone effect.

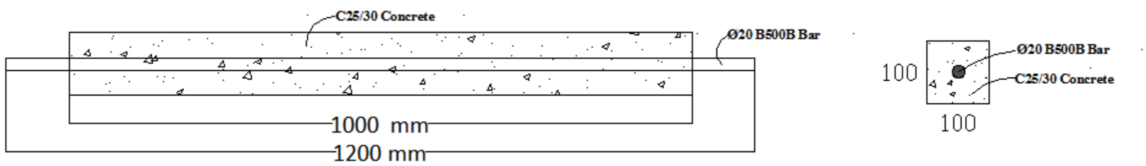

Figure 3-8: Diameter 20 B500B bar embedded in 100x100mm

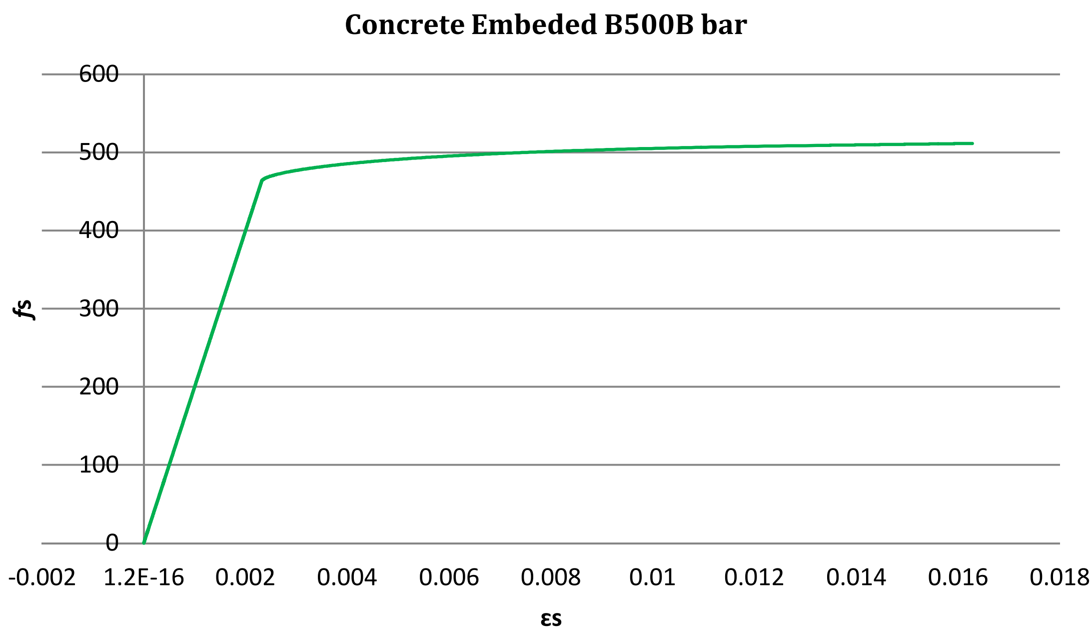

Figure 3-9: Stress vs. strain diagram of bare reinforcing bar under tension

The relationship between the steel stress and the average stress of the bar and concrete is plotted by using Eq. 3.1.

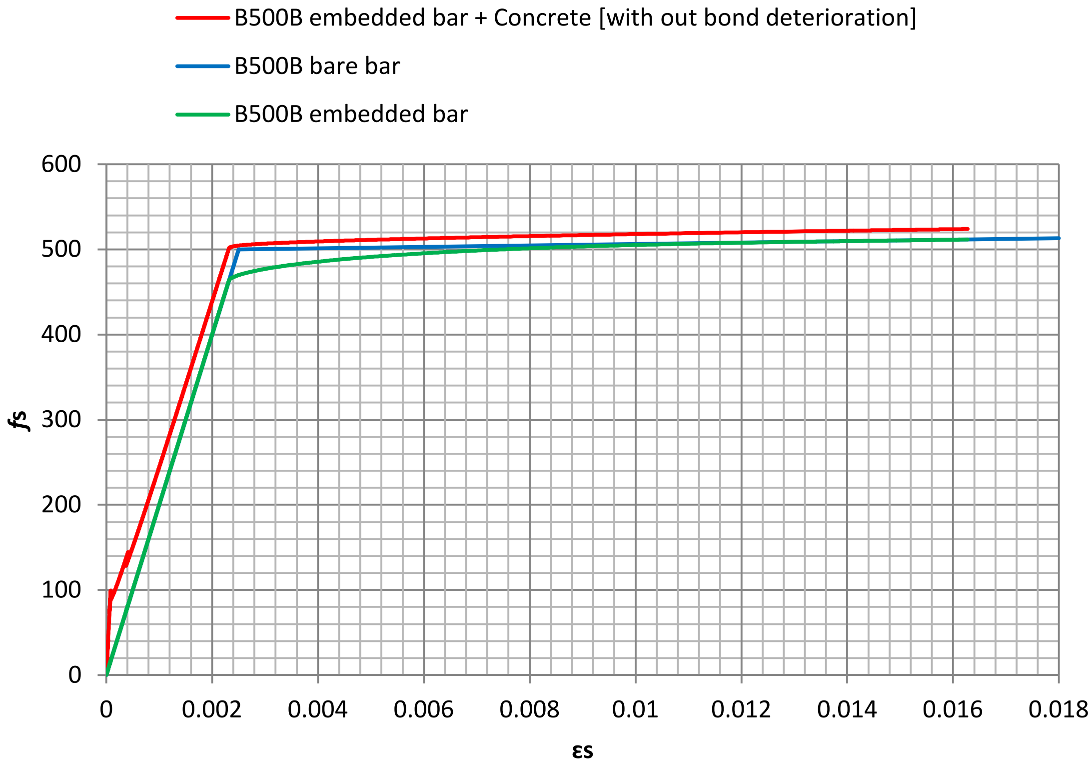

Figure 3-10: Comparison of the three stress vs. strain diagram in the tension zone.

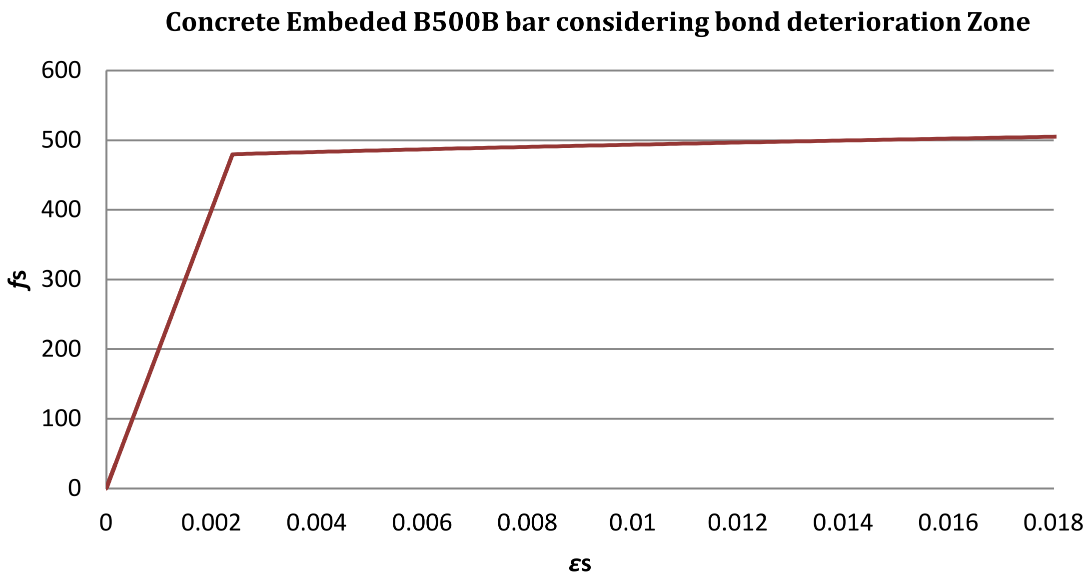

Figure 3-11: Stress vs. strain diagram of bare reinforcing bar under tension considering bond deterioration zone.

Similarly the relationship between the steel stress and the average stress of the bar and concrete considering tension stiffening and bond deterioration zone is plotted by using Eq. 3.1.

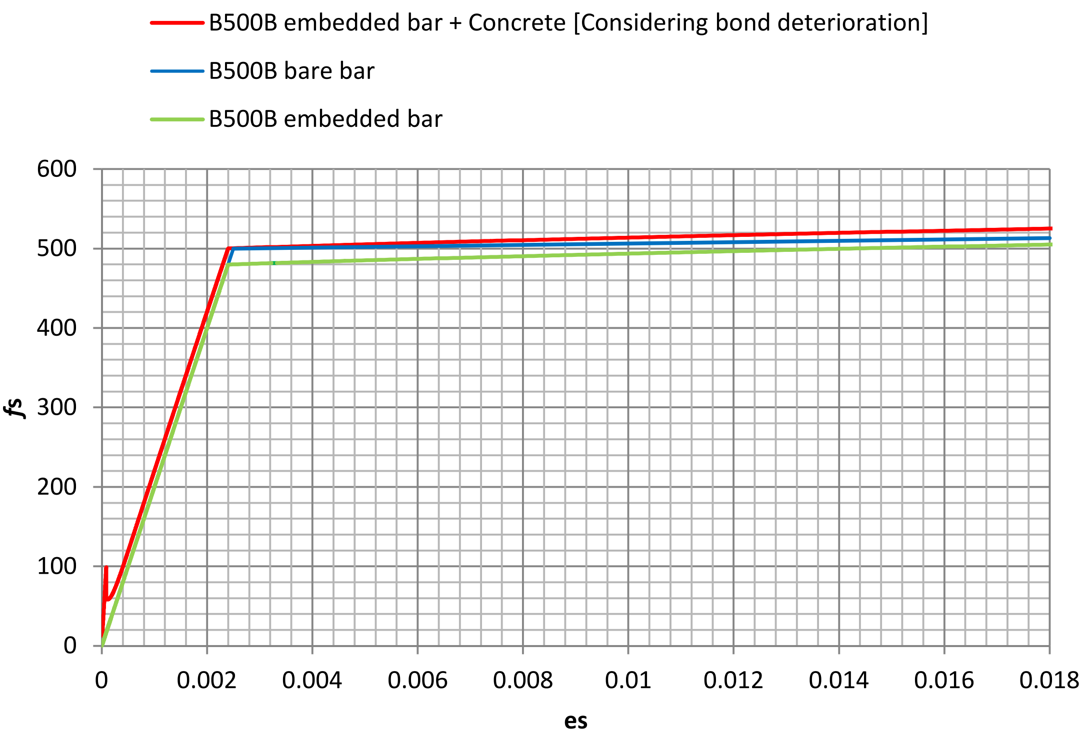

Figure 3-12: Comparison of the three stress vs. strain diagram in the tension zone considering bond deterioration zone.

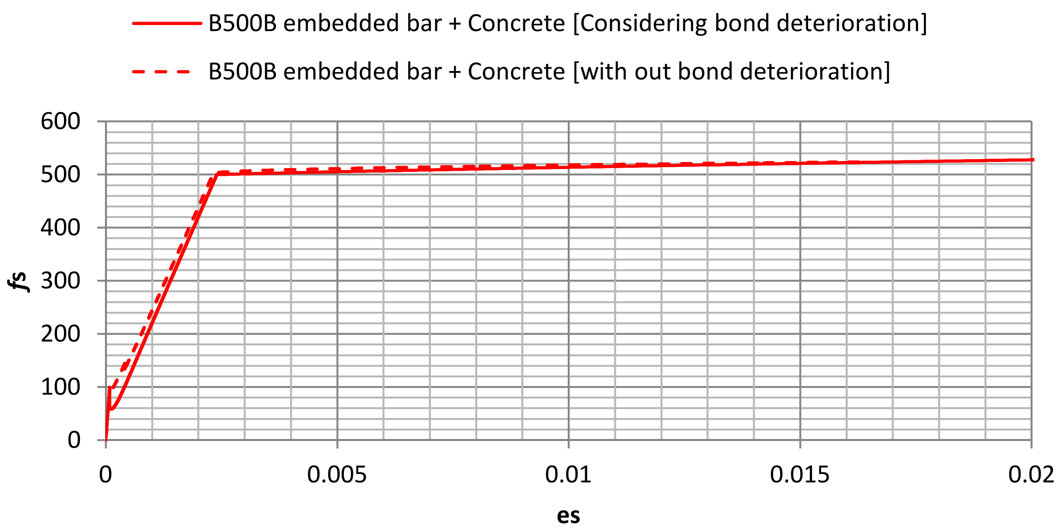

Figure 3-13: Comparison of the stress vs. strain diagram in the tension zone a. without bond deterioration zone b. considering bond deterioration zone

The impact of the bond deterioration area on stress and strain diagram of the embedded bar is shown in Figure 3-13. The dashed line represents a graph by considering only tension stiffening. The Stress vs. strain graph has three characteristics. Those are before cracking, after cracking and after yielding of the reinforcement. The first part which has higher slop is before crack start. As the graph represent before crack both stress are the same. The second part is after crack start. The graph that considers the loss of bond has a lower slop. This gives a lower fully cracked secant modulus.

It is observed in these figures that the impact of tension stiffening and bond deterioration zone has an effect on the behavior of stress vs. strain. This is not well incorporated in the design code methods. As disused in the literature review, by incorporating the coefficient β, Euro code includes the impact of tension stiffening. But in all design codes, the impact of bond deterioration is not well integrated.

The initial slope of proposed curve is significantly larger than the one used in codes this will definitely have an exaggerated difference in the deflection calculation. The author has realized that, it is unrealistic to consider the whole concrete section below the neutral axis having the same influence on the reinforcement embedded. In this research, the effective zone has taken as proposed in (CEP-FIP, 1978). The reason behind this is to clearly see the effect of intact concrete between cracks. Accordingly the beam will have the following effective embedment zone.

$$C_d = 7.5 \times Diameter\ of\ the\ bar = 7.5 \times 24 = 180\ mm$$

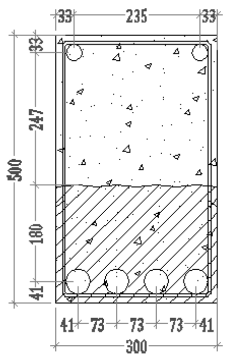

Figure 3-14: Proposed effective reinforced concrete section in the tension zone.

As discussed in section 2.4.1, (Tadesse, 2015) evaluate a simple supported beam's short-term deflection. Hear under deflection is calculated by considering tension stiffening and bond deterioration zone.

3.4 Calculation of Short-term deflection Introducing Tension Stiffening

3.4.1 Design Data

G_k = 18.75 kN/m

Q_k = 15 kN/m

A'_s = 402 mm^2 (2ϕ16)

A_s = 1810 mm^2 (4ϕ24)

f_c = 25 N/mm (concrete strength class C25/30)

f_s= 435 N/mm (Steel B435B)

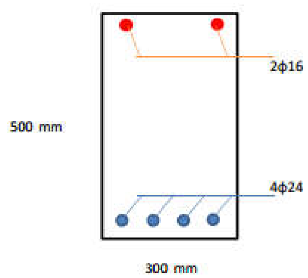

Figure 3-15: Cross-Section

3.4.2 Stress vs. Strain diagram

The stress vs. strain diagram of the beam is calculated by using the code provides in Appendix A.

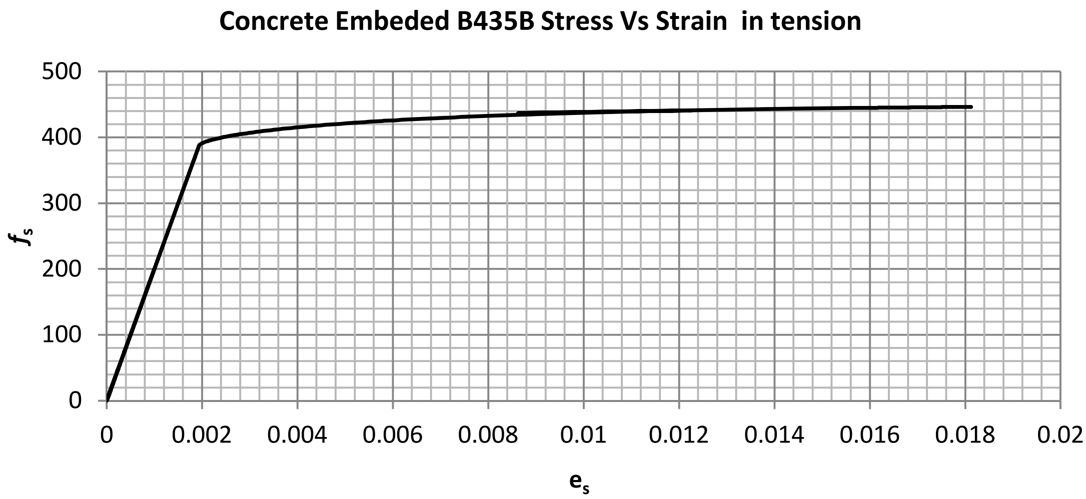

Figure 3-16: Stress vs. strain diagram proposed effective reinforced concrete section in the tension zone.

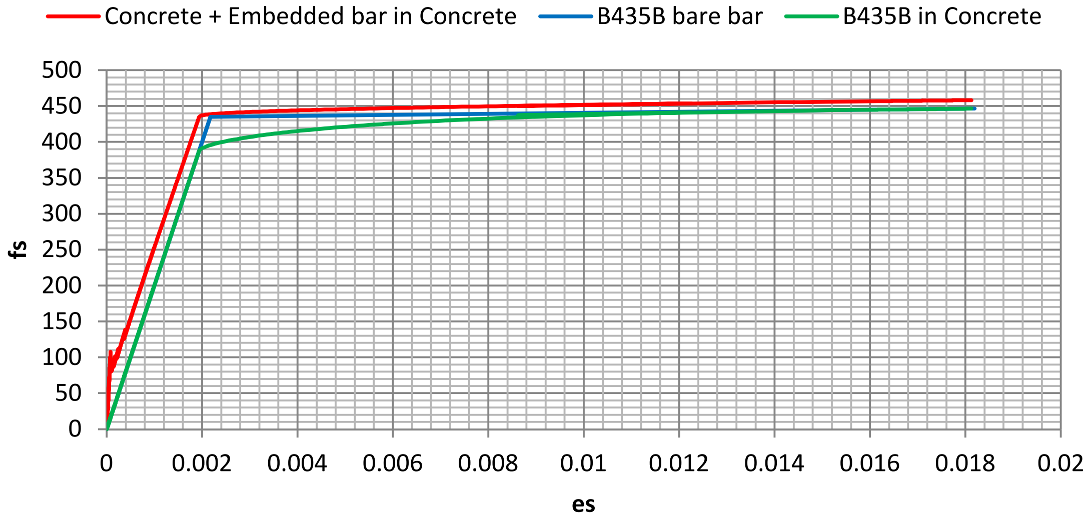

Figure 3-17: Comparison of the three stress vs. strain diagram in tension for the proposed effective concrete section in the tension.

3.4.3 Calculation of Moments

The quasi-permanent combination of loading is given, for one variable action, by

$G_k + \psi_2 Q_k$ Where $\psi_2 = 0.3$

Therefore Loading =18.75+(0.3*15)=23.25kN/m

$$Mid - span\ bending\ moment\ (M) = \frac{23.25\ x\ 7^2}{8} = 142.41\ kNm$$

3.4.4 Calculation of Curvatures

Only the curvature of flexibility is calculated. Shrinkage and creep effect is ignored. In order to calculate the curvatures, the properties of the uncracked and cracked sections must first be calculated and the moment at which cracking occurs must be determined.

For the concrete strength Class C25/30, E_{cm}=31kN/mm^2

For fully cracked section steel strength Class B435B, E_s=343.93 kN/mm^2

$$\text{Effective modular ratio } (\alpha_e) = \frac{E_s}{E_{c,eff}} = \frac{343.93}{31} = 11.094$$

3.4.4.1 UNCRACKED TRANSFORMED SECTION

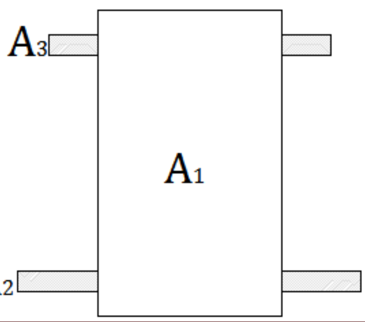

Figure 3-18: Un-cracked transformed section

Neutral axis depth of the uncracked section

Part A_i	A [mm2]	y [mm]	Ay [mm3]
1	150000	250	37500000
2	18270.9574	455	8313285.6
3	4057.96955	45	182608.63
∑	172328.927		45995894

$$\bar{y} = \frac{\sum Ay}{A} = \frac{45995894}{172328.927} = 266.91\ mm$$

The second moment of the area of the cracked section

Part A_i	A [mm²]	I [mm⁴]	Y_{bar} [mm]	$A^*y_{bar}^2$ [mm⁴]
1	150000	149377749	90.73	448133247
2	18270.9574	0	-273.54	1502535331
3	4057.96955	0	136.46	75565287.47
∑	172328.927	3125000000		2026233866

$$I_{un} = 3125000000 + 2026233866 = 4014110218\ \text{mm}^4$$

3.4.4.2 *CRACKED TRANSFORMED SECTION*

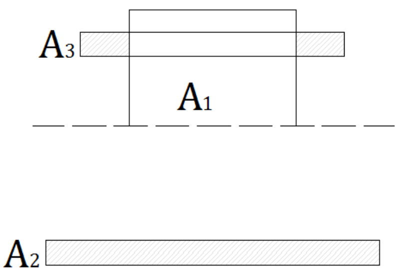

Figure 3-19: cracked transformed section

Neutral axis depth of the cracked section

$$k_x = \frac{x}{d} = -\alpha_e\rho + (\alpha_e - 1)\rho' + \sqrt{[\alpha_e\rho + (\alpha_e - 1)\rho']^2 + 2[\alpha_e\rho + (\alpha_e - 1)\rho']\frac{d'}{d}}$$

$$x = 0.327d = 181.46\ mm$$

The second moment of the area of the cracked section

Part A_i	A [mm^2]	I [mm^4]	Y_{bar} [mm]	A*$ybar^2$ [mm^4]
1	54438.13	149377749	90.73022162	448133247
2	20080.96	0	-273.5395568	1502535331
3	4057.97	0	136.4604432	75565287.47
∑	78577.06	129109770		2026233866

$$I_{cr} = 129109770 + 2026233866 = 2175611615 \text{ mm}^4$$

3.4.4.3 Flexural Cracking Moment

$$\mathrm{M_{cr}} = \frac{f_{\mathrm{ctm}}\mathrm{I_{un}}}{\mathrm{y_t}}$$

Where: for concrete strength grade C25/30, f_{ctm} =2.6 N/mm

y_t = h-x = 500-266.91 = 233.09 mm

$$\mathrm{M_{cr}} = \frac{f_{\mathrm{ctm}}\mathrm{I_{un}}}{\mathrm{y_t}} = \frac{2.6 * 4014110218}{233.09} = 44.77 \text{ kNm}$$

The section has cracked, since $M_{cr} < M$

3.4.4.4 CURVATURE OF THE UNCRACKED SECTION

$$\varphi_{\mathrm{un}} = \frac{\mathrm{M}}{\mathrm{E_{c,eff}I_{un}}} = \frac{142.41 * 10^6}{31 * 10^3 * 4014110218} = 1.14 * 10^{-6}\ {}^{\mathrm{rad}}/_{\mathrm{mm}}$$

3.4.4.5 CURVATURE OF THE CRACKED SECTION

A linear strain distribution is assumed, as shown in Figure 3-20 b, The exact magnitude of that stress and strain in tension is known, and thus, the depth to the neutral axis, c, can be computed. The following relationship can be established from similar triangles in the strain diagram:

$$\frac{e'_s}{c-d'} = \frac{e_{cm}}{c} \quad or \quad e'_s = \frac{(c-d')}{c} e_{cm} \qquad \text{Eq. 3.11}$$

$$\varepsilon_{cm} = \frac{\varepsilon_s}{\left(\frac{d}{y} - 1\right)} \qquad \text{Eq. 3.12}$$

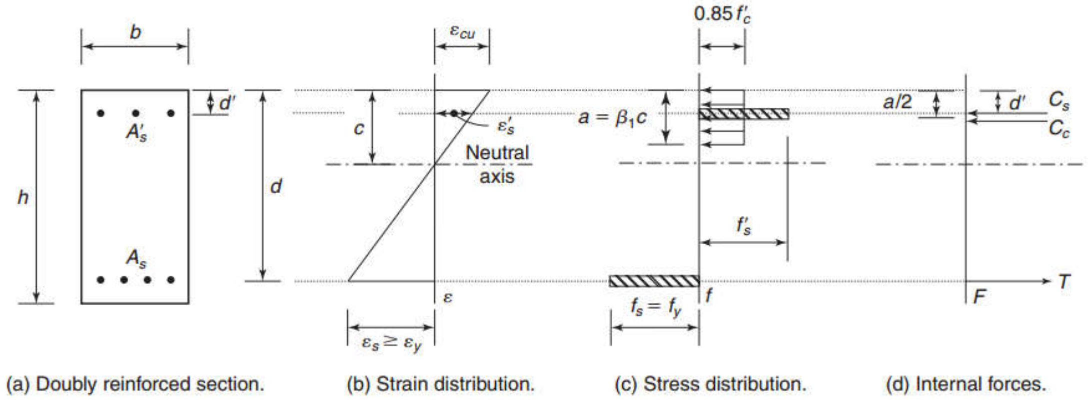

Figure 3-20: Stress and Strain distribution

The assumed distribution of stresses is shown in Figure 3-20 c. As before, the real concrete compression stress distribution is replaced by Whitney's stress block. The stress in the compression reinforcement is not known and cannot be determined until the depth to the neutral axis has been determined. The internal section forces are shown symbolically in Figure 3-20 d. The concrete compression force, is assumed to be the same as:

$$C_c = 0.8f'_c yb = 0.8f'_c yb \quad \text{Eq. 3.13}$$

The force in the compression reinforcement is expressed as

$$C_s = A'_s f'_s = A'_s E_s \varepsilon'_s \quad \text{Eq. 3.14}$$

The tension force is simply the area of tension reinforcement multiplied by the steel stress.

$$T_s = A_s f_s \quad \text{Eq. 3.15}$$

Thus, establishing section equilibrium results in the following:

$$T_s = C_C + C_s$$
$$A_s f_s = A'_s f'_s + 0.8f'_c yb \quad \text{Eq. 3.16}$$

In this expression, there are three unknowns: the neutral axis depth, c, the stress in the compression reinforcement, and the concrete compression force, f_c', The compression steel stress can be assumed to be linearly related to the compression steel strain, as expressed in Eq. 3.14. Also, the compression steel strain is linearly related to the neutral axis depth given in Eq. 3.16.

To get Concrete Compression strength , f_c', we can use

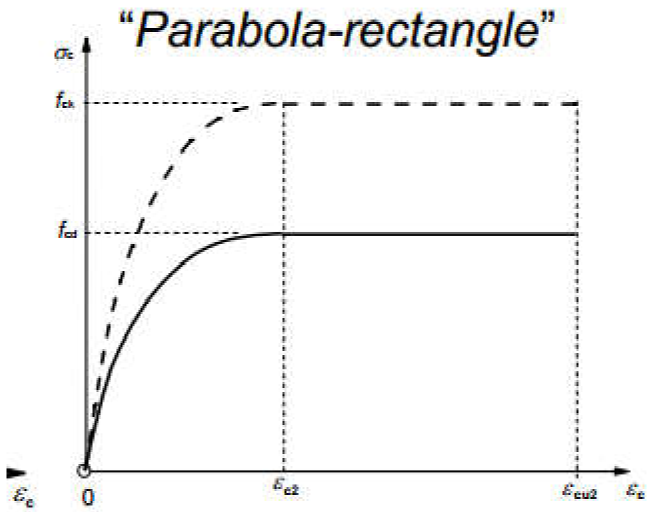

Figure 3-21: parabola – rectangle stress and strain distribution of concrete

$$\sigma_c = f_{ck}\left[1-\left(\frac{\varepsilon_c}{\varepsilon_{c2}}\right)^n\right] \quad for\ 0 \le \varepsilon_c < \varepsilon_{c2}$$

$$\sigma_c = f_{ck} \quad for\ \varepsilon_{c2} \le \varepsilon_c \le \varepsilon_{cu2}$$

Where $n = 1.4 + 23.4\left[\frac{90-f_{ck}}{100}\right]^4\ for\ f_{ck} \ge 50\ Mpa\ otherwise\ 2$ Eq. 3.17

$$\varepsilon_{c2}\left({}^{0}/_{00}\right) = 2 + 0.085(f_{ck}-50)^{0.63} for\ f_{ck} \ge 50\ Mpa\ otherwise\ 2$$

$$\varepsilon_{cu2}\left({}^{0}/_{00}\right) = 2.6 + 35\left[\frac{90-f_{ck}}{100}\right]^4\ for\ f_{ck} \ge 50\ Mpa\ otherwise\ 3.5$$

$$\sigma_c = f_{ck}\left[1-\left(\frac{\varepsilon_s/\left(\frac{d}{y}-1\right)}{0.002}\right)^n\right] \qquad \text{Eq. 3.18}$$

Therefore compression force can be rewritten as follow

$$C_c = 0.8f'_c yb = 0.8ybf_{ck}\left[1-\left(\frac{\varepsilon_s/\left(\frac{d}{y}-1\right)}{0.002}\right)^2\right]$$

Taking the stress and strain in the tension reinforcement from the stress strain graph, f_s & ε_s. Thus, the section equilibrium expressed in Eq. 3.16 will be converted to a quadratic equation in terms of one unknown, y.

For the analysis presented here, that point is taken at the level of the tension reinforcement. Thus, T is eliminated from the calculation and the resulting expression for is

$$M = C_c(d - 0.4y) + C_s(d - d') \qquad \text{Eq. 3.19}$$

Steel stress for fully cracked section:

$$f_s = \frac{M}{A_s(d - {}^{x}/_{3})} = \frac{142.41 * 10^6}{1810(455 - {}^{181.46}/_{3})} = 199.43 \text{ Mpa}$$

$$\varphi_{cr} = \frac{\varepsilon}{d-x} = \frac{E_s}{f_s(455-x)} = \frac{343.93}{199.43*(455-18\ 146)} = 2.12 * 10^{-6}\ {}^{rad}/_{mm} \text{ or}$$

$$\varphi_{cr} = \frac{M}{E_{c,eff} I_{cr}} = \frac{142.41 * 10^6}{31 * 10^3 * 2175611615} = 2.12 * 10^{-6}\ {}^{rad}/_{mm}$$

The steel stress for Maximum Moment.

To calculate the neutral axis depth we can use the above equations

$$T_s = C_C + C_s$$
$$A_s f_s = A'_s f'_s + 0.8 f'_c y b$$

$$1810 * f_s = 402 * 200 * \frac{(y - d')}{y} * \frac{\varepsilon_s}{\left(\frac{455}{y} - 1\right)} + 0.8 * 300 * 25 * y * \left[1 - \left(\frac{{}^{\varepsilon_s}/\left(\frac{455}{y} - 1\right)}{0.002}\right)^2\right]$$

Taking the stress and strain in the tension reinforcement from the stress strain graph, f_s = 200.335 Mpa & ε_s = 0.00073. Thus, the section equilibrium will be converted to a quadratic equation in terms of one unknown, y.

$$1810 * 200.335 = 402 * 200 * \frac{(y - 41)}{y} * \frac{0.00073}{\left(\frac{455}{y} - 1\right)} + 0.8 * 300 * 25 * c * \left[1 - \left(\frac{{}^{0.00073}/\left(\frac{455}{y} - 1\right)}{0.002}\right)^2\right]$$

$$y = 159.358 \text{ mm}$$

Concrete Compression force:

$$C_c = 0.8 * 184.1342 * 300 * 25 * \left[1 - \left(\frac{{}^{0.00073}/\left(\frac{455}{159.358} - 1\right)}{0.002}\right)^2\right] = 339117.4 \text{ Mpa}$$

Tension bar force:

$$C_s = A'_s E_s \varepsilon'_s = 402 * 200 * \frac{(159.358 - 41)}{159.358} * \frac{0.00073}{\left(\frac{455}{159.358} - 1\right)} = 23488.81 \text{ Mpa}$$

Moment:

$$M = C_c(d - 0.4c) + C_s(d - d')$$
$$= 339117.4 * (455 - 0.4 * 159.358) + 23488.81 * (455 - 41)$$
$$= 142.4064 \text{ kNm}$$

Similarly for f_s= 200.3756 Mpa and ε_s= 0.00073 : y= 159.355 mm and M= 142.4357 kNm . By interpolating this values for M= 142.41 kNm: Y=159.3576 mm, f_s= 200.34 Mpa and ε_s= 0.00073

Curvature at M= 142.41 kNm:

$$\varphi = \frac{\varepsilon}{d - x} = \frac{0.00073}{455 - 159.3576} = 2.468 * 10^{-6} \text{ rad}/\text{mm}$$

3.4.4.6 Total Curvature and Deflection

Here below is the tabulated result for curvature and deflection along the span on the beam

Table 3-1: Deflection Calculation of the above beam considering Tension stiffening and bond deterioration zone

X/L	M. [kN/m]	X [mm]	ε [10^{-4}]	1/r[* 10^{-6} rad/ mm]	1St integral [10^3 rad]	2nd integral [10^3mm]	Correction	Deflection [mm]
0.00	0.00	266.908	0	0.000	0.00	0.0	0.0	0.000
0.05	27.06	266.908	-	0.217	0.04	0.0	1.8	-1.748
0.10	51.27	267.055	0.629	0.335	0.13	0.0	3.5	-3.473
0.20	91.14	175.690	3.55	1.270	0.70	0.3	7.0	-6.692
0.30	119.62	162.707	5.73	1.959	1.83	1.2	10.5	-9.319
0.40	136.71	160.049	6.90	2.340	3.33	3.0	14.0	-11.024
0.50	142.41	159.358	7.30	2.468	5.01	5.9	17.5	-11.613
0.60	136.71	160.049	6.90	2.340	6.70	10.0	21.1	-11.024
0.70	119.62	162.707	5.73	1.959	8.20	15.3	24.6	-9.319
0.80	91.14	175.690	3.55	1.270	9.33	21.4	28.1	-6.692
0.90	51.27	267.055	0.629	0.335	9.89	28.1	31.6	-3.473
0.95	27.06	266.908	-	0.217	9.99	31.6	33.3	-1.748
1.00	0.00	266.908	0	0.000	10.03	35.1	35.1	0.000

3.5 Calculation of Short-term Deflection By Introducing Bond Deterioration Zone on Tension Stiffening

As mentioned in section 2.2.5, concrete continues to carry a tension between cracks by transferring bond forces from the reinforcing bars into the concrete. However, due to the splitting and crushing of concrete around the bar, the bond force will deteriorate. This effect is called bond deterioration zone, and under service load conditions this phenomenon has an effect on the stiffness of the member, deflection and crack widths.

3.5.1 Stress vs. Strain diagram

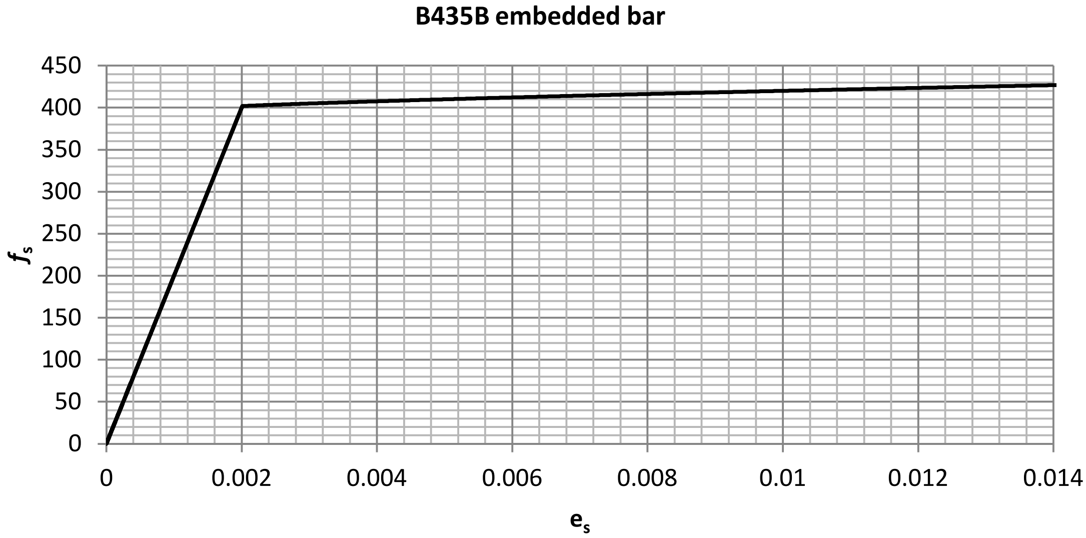

Figure 3-22: Stress vs. strain diagram proposed effective reinforced concrete section in the tension zone.

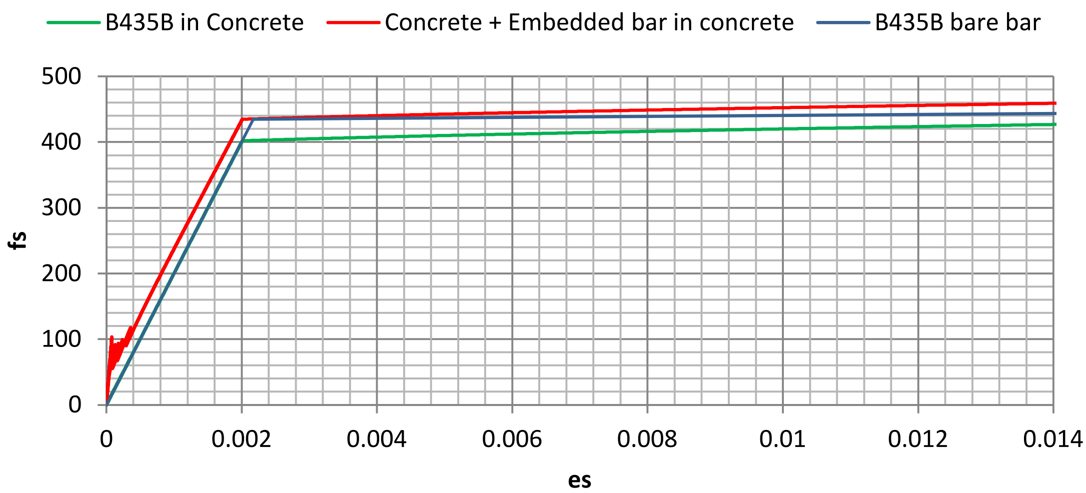

Figure 3-23: Comparison of the three stress vs. strain diagram in tension for the proposed effective concrete section in the tension zone.

3.5.2 Calculation of Curvatures

Only the curvature of flexibility is calculated. Shrinkage and creep effect is ignored. In order to calculate the curvatures, the properties of the uncracked and cracked sections must first be calculated and the moment at which cracking occurs must be determined.

For the concrete strength Class C25/30, E_{cm}=31kN/mm^2

For fully cracked section steel strength Class B435B, E_s=299.02 kN/mm^2

Effective modular ratio $(\alpha_e) = \frac{E_s}{E_{c,eff}} = \frac{299.02}{31} = 9.64$

3.5.2.1 UNCRACKED TRANSFORMED SECTION

The neutral axis depth and the uncracked second moment of inertia are of the same value as calculated in section 3.4.4.1 and summarized below:

$\bar{y} = 264.76\, mm$

$I_{un} = 3891885260\ \text{mm}^4$

3.5.2.2 CRACKED TRANSFORMED SECTION

Neutral axis depth and second moment of the area of the fully cracked section are of the same value as calculated in section 3.4.4.2 and summarized below:

$x = 172.85\, mm$

$I_{cr} = 1963116890\ \text{mm}^4$

3.5.2.3 FLEXURAL CRACKING MOMENT

$$\mathrm{M_{cr}} = \frac{f_{\mathrm{ctm}}\mathrm{I_{un}}}{\mathrm{y_t}}$$

Where: for concrete strength grade C25/30, f_{ctm} =2.6 N/mm

y_t = h-x = 500-264.76 = 235.24 mm

$$\mathrm{M_{cr}} = \frac{f_{\mathrm{ctm}}\mathrm{I_{un}}}{\mathrm{y_t}} = \frac{2.6 * 3891885260}{235.24} = 43.01\ \mathrm{kNm}$$

The section has cracked, since $M_{cr} < M$

3.5.2.4 CURVATURE OF THE UNCRACKED SECTION

$$\varphi_{un} = \frac{M}{E_{c,eff} I_{un}} = \frac{142.41 * 10^6}{31 * 10^3 * 3891885260} = 1.18 * 10^{-6}\,{}^{rad}/_{mm}$$

3.5.2.5 CURVATURE OF THE CRACKED SECTION

Steel stress for fully cracked section:

$$f_s = \frac{M}{A_s(d - {}^{x}/_{3})} = \frac{142.41 * 10^6}{1810(455 - {}^{172.85}/_{3})} = 197.99 \text{ Mpa}$$

$$\varphi_{cr} = \frac{\varepsilon}{d - x} = \frac{E_s}{f_s(455 - x)} = \frac{299.02}{197.99 * (455 - 172.85)} = 2.34 * 10^{-6}\,{}^{rad}/_{mm}$$

$$\varphi_{cr} = \frac{M}{E_{c,eff} I_{cr}} = \frac{142.41 * 10^6}{31 * 10^3 * 1963116890} = 2.34 * 10^{-6}\,{}^{rad}/_{mm}$$

Steel stress for Maximum Moment:

The neutral axis depth is calculated as discussed in section 3.4.4.5. Taking the stress and strain in the tension reinforcement from the stress strain graph, f_s = 199.119 Mpa & ε_S = 0.000808. : y= 152.8465 mm and M= 142.338 kNm

Similarly for f_s= 199.119 Mpa and ε_S= 0.000807 : y= 152.846 mm , M= 142.434 kNm

By interpolating this values for M= 142.41 kNm: Y=152.8478 mm, f_s= 199.08 Mpa and ε_S= 0.000808

$$\varphi_{M=142.41} = \frac{\varepsilon}{d - x} = \frac{0.000807}{455 - 152.8478} = 2.67 * 10^{-6}\,{}^{rad}/_{mm}$$

3.5.2.6 Total Curvature and Deflection

Here below is the tabulated result for curvature and deflection along the span on the beam

Table 3-2: Deflection Calculation of the above beam considering Tension stiffening and bond deterioration zone

X/L	M. [kN/m]	X [mm]	ε [10^{-4}]	*Φ* [10^{-6} rad/mm]	1St integral [10^3 rad]	2nd integral [10^3mm]	Correction	Deflection [mm]
0.00	0.00	264.756	0	0.000	0.00	0.0	0.0	0.000
0.05	27.06	264.756	-	0.224	0.04	0.0	1.9	-1.929
0.10	51.27	317.676	0.345	0.252	0.12	0.0	3.9	-3.836
0.20	91.14	157.432	4.63	1.555	0.75	0.3	7.7	-7.401
0.30	119.62	154.283	6.51	2.165	2.06	1.3	11.6	-10.288
0.40	136.71	153.136	7.68	2.544	3.71	3.3	15.5	-12.143
0.50	142.41	152.848	8.07	2.672	5.53	6.6	19.4	-12.782
0.60	136.71	153.136	7.68	2.544	7.36	11.1	23.2	-12.143
0.70	119.62	154.283	6.51	2.165	9.00	16.8	27.1	-10.288
0.80	91.14	157.432	4.63	1.555	10.31	23.6	31.0	-7.401
0.90	51.27	317.676	3.45	0.252	10.94	31.0	34.8	-3.836
0.95	27.06	264.756	-	0.224	11.02	34.9	36.8	-1.929
1.00	0.00	264.756	0	0.000	11.06	38.7	38.7	0.000

3.6 Comparison

Table 3-3: Summary of the deflection calculation

x	δ ACI [mm]	δ ACI - EC2 [mm]	Bischoff's [mm]	δ EC2 [mm]	δ proposed method considering tension stiffening [mm]	δ proposed method considering tension stiffening and Bond deterioration Zone [mm]	Difference with proposed method considering tension stiffening [%]	Difference with proposed method considering tension stiffening and Bond deterioration Zone [%]
0.0	0.000	0.000	0.000	0.000	0.000	0.000	0.00	0.00
0.7	-2.364	-3.045	-2.731	-4.535	-3.473	-3.836	23.41	15.40
1.4	-7.976	-8.586	-8.722	-8.667	-6.692	-7.401	22.79	14.61
2.1	-12.06	-12.494	-12.887	-11.96	-9.319	-10.288	22.09	13.99
2.8	-14.52	-14.878	-15.452	-14.07	-11.024	-12.143	21.65	13.70
3.5	-15.35	-15.685	-16.322	-14.79	-11.613	-12.782	21.51	13.61
4.2	-14.52	-14.878	-15.452	-14.07	-11.024	-12.143	21.65	13.70
4.9	-12.06	-12.494	-12.887	-11.96	-9.319	-10.288	22.09	13.99
5.6	-7.976	-8.586	-8.722	-8.667	-6.692	-7.401	22.79	14.61
6.3	-2.364	-3.045	-2.731	-4.535	-3.473	-3.836	23.41	15.40
7.0	0.000	0.000	0.000	0.000	0.000	0.000	0.00	0.00

As the results imply the deflection is significantly small when calculated considering the role of concrete still intact between consecutive cracks. However the proposed method, which includes bond deterioration zone on tension stiffening, provides the closest outcome than the deflection technique that ignores the bond deterioration zone impact.

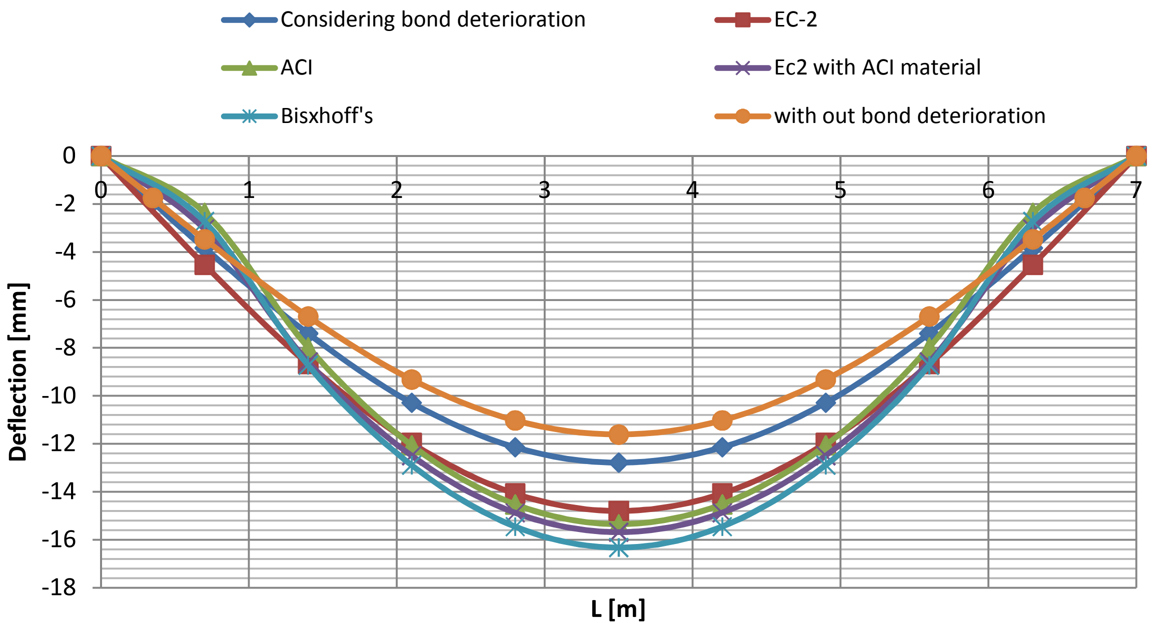

Figure 3-24: Deflection Curve

4. EXPERMENTAL VERIFICATION

As expressed in the analysis, the stress vs strain graph of the embedded bar has three characteristics. Those are before cracking, after cracking and after yielding of the reinforcement. The researcher has taken loads so as to check and verify the deflection values. The rationale behind choosing the loads is to clearly indicate the behaviors before yielding of the reinforcement. The loads clearly show the three behaviors before cracking, after cracking and before yielding of the reinforcement.

4.1 Deflection calculation of Specimen B2M

From the experimental result of the research Fatigue behavior of shear-critical reinforced concrete beams (Getachew, 2018), Specimen B2M is used to verify the proposed method of calculation of deflection. This beam is tested under a monotonically increasing load, 63 days after casting. From the experimental result the cube compression strength is 31.98 N/mm, tensile strength is 2.403 N/mm and steel yield strength of 603.47 N/mm. The cross section of the beam is shown in Figure 4-1.

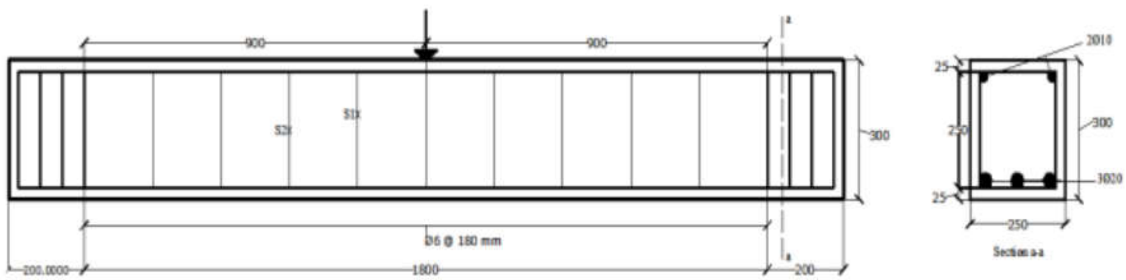

Figure 4-1: Specimen B2M (Getachew, 2018)

4.1.1 Calculation of Short Term Deflection in Accordance to EC-2

Deflections will be calculated using the rigorous method given in EC2.

- For the concrete strength of 31.98 N/mm, E_{cm}=32472 N/mm^2
- For fully cracked section steel strength of 603.47 N/mm, Es=200 kN/mm^2
- Effective modular ratio $(\alpha_e) = \frac{E_s}{E_{c,eff}} = \frac{200}{32.47\ 2} = 6.159$

4.1.1.1 UNCRACKED TRANSFORMED SECTION

In the same method as in section 3.4.4.1, neutral axis depth and second moment of inertia are calculated as follows:

$\bar{y} = 154.257\ mm$

$I_{un} = 635249679.6\ \text{mm}^4$

4.1.1.2 CRACKED TRANSFORMED SECTION

In the same method as in section 3.4.4.1, neutral axis depth and second moment of inertia of the fully cracked section are calculated as follows:

$x = 85.95\ mm$

$I_{cr} = 225741879.5\ \text{mm}^4$

4.1.1.3 FLEXURAL CRACKING MOMENT

$$\text{M}_{\text{cr}} = \frac{f_{\text{ctm}}\text{I}_{\text{un}}}{\text{y}_{\text{t}}} = \frac{2.403 * 635249679.6}{300 - 154.257} = 10.47\ \text{kNm}$$

4.1.1.4 CALCULATION OF DEFLECTION

- For 20 kN load

$$Mid - span\ bending\ moment\ (M) = \frac{20\ x\ 1.8}{4} = 9\ kNm$$

:- The section has not cracked, since $M_{cr} > M$

$$\delta = -\frac{PL^3}{48E_cI_e} = -\frac{20 * 1800^3}{48 * 32472 * 635249679.6} = -0.117\ mm$$

- For 50 kN load

$$Mid - span\ bending\ moment\ (M) = \frac{50\ x\ 1.8}{4} = 22.5\ kNm$$

:- the section has cracked, since $M_{cr} < M$

Here below is the tabulated result for curvature along the span on the beam

Table 4-1: Total curvature in accordance to EC2 ($*10^{-6}$ rad/mm)

X/L	Moment [kN/m]	$1/r_{un}$	$1/r_{cr}$	ζ	1/r	$1/r_{cs}$	$1/r_{tot}$
0.00	0.00	0.000	0.000	0.000	0.000	0.000	0.000
0.10	4.50	0.218	0.614	0.000	0.218	0.000	0.218
0.20	9.00	0.436	1.228	0.000	0.436	0.000	0.436

0.30	13.50	0.654	1.842	0.398	1.127	0.000	1.127
0.40	18.00	0.873	2.456	0.661	1.920	0.000	1.920
0.50	22.50	1.091	3.069	0.783	2.641	0.000	2.641
0.60	18.00	0.873	2.456	0.661	1.920	0.000	1.920
0.70	13.50	0.654	1.842	0.398	1.127	0.000	1.127
0.80	9.00	0.436	1.228	0.000	0.436	0.000	0.436
0.90	4.50	0.218	0.614	0.000	0.218	0.000	0.218
1.00	0.00	0.000	0.000	0.000	0.000	0.000	0.000

Having calculated the total curvatures, the deflections may be calculated by numerical integration using the trapezoidal rule. The uncorrected rotation at any point may be obtained by the first integral given by

$$\theta_x = \theta_{x-1} + \left(\frac{{}^1/_{r_x} + {}^1/_{r_{x-1}}}{2} \right) \times \frac{L}{n} \qquad \text{Eq. 4. 1}$$

Having calculated the uncorrected rotations, the uncorrected deflections may be obtained by the second integral given by:

$$\delta_x = \delta_{x-1} + \left(\frac{\theta_x + \theta_{x-1}}{2} \right) \times \frac{L}{n} \qquad \text{Eq. 4. 2}$$

Where: the subscript x denotes the values of the parameters at the fraction of the span being considered, and the subscript x-1 denotes the values of the parameters at the preceding fraction of the span. L is the span length and n is the number of the span divisions considered.

The values of the uncorrected rotations, uncorrected and corrected deflections at positions x/l along the span are given in Table 4-2.

Table 4-2: Deflections in accordance to EC2 [mm]

X/L	**1st integral [10³ rad]**	**2nd integral [10³ mm]**	**Correction**	**Deflection**
0.00	0.000	0.000	0.000	0.000
0.10	0.020	0.002	0.163	-0.161
0.20	0.079	0.011	0.325	-0.315
0.30	0.219	0.037	0.488	-0.451
0.40	0.493	0.102	0.651	-0.549
0.50	0.904	0.227	0.813	**-0.586**
0.60	1.314	0.427	0.976	-0.549
0.70	1.588	0.688	1.139	-0.451
0.80	1.729	0.987	1.302	-0.315
0.90	1.788	1.303	1.464	-0.161
1.00	1.808	1.627	1.627	0.000

- For 50 kN load the section has cracked, since $M_{cr} < M$

$$Mid - span\ bending\ moment\ (M) = \frac{250\ x\ 1.8}{4} = 112.5\ kNm\ ; p = 250\ kN$$

:- the section has cracked, since $M_{cr} < M$

In the same method, curvature and deflection along the span are calculated as follows:

Table 4-3: Total curvature and deflection in accordance to EC2 (*10^{-6} rad/mm)

X/L	Moment [kN/m]	$1/r_{un}$	$1/r_{cr}$	ζ	$1/r_{tot}$	1st integral [10^3 rad]	2nd integral [10^3mm]	Correction	Deflection
0.0	0.00	0.000	0.000	0.000	0.000	0.000	0.000	0.000	0.000
0.1	22.50	1.091	3.069	0.783	2.641	0.238	0.021	1.213	-1.191
0.2	45.00	2.182	6.139	0.946	5.925	1.009	0.134	2.426	-2.292
0.3	67.50	3.272	9.208	0.976	9.065	2.358	0.437	3.638	-3.202
0.4	90.00	4.363	12.278	0.986	12.171	4.269	1.033	4.851	-3.818
0.5	112.50	5.454	15.347	0.991	15.262	6.738	2.023	6.064	**-4.041**
0.6	90.00	4.363	12.278	0.986	12.171	9.207	3.458	7.277	-3.818
0.7	67.50	3.272	9.208	0.976	9.065	11.118	5.288	8.490	-3.202
0.8	45.00	2.182	6.139	0.946	5.925	12.467	7.410	9.702	-2.292
0.9	22.50	1.091	3.069	0.783	2.641	13.238	9.724	10.915	-1.191
1.0	0.00	0.000	0.000	0.000	0.000	13.476	12.128	12.128	0.000

4.1.2 Calculation of Short Term Deflection in Accordance to ACI-318

For calculation of immediate deflections of uncracked prismatic members, the usual methods or formulas for elastic deflections may be used with a constant value of E_cI_g along the length of the member. However, if the member is cracked at one or more sections, or if its depth varies along the span, a more exact calculation becomes necessary. The ACI 318 technique is based on the method proposed by Branson, which uses the effective moment of inertia as expressed in Eq 2.11.

- For the concrete strength of 31.98 N/mm, $E_{cm} = 4500\sqrt{31.98} = 25.45$kN/mm^2
- For fully cracked section steel strength of 603.47, E_s=200 kN/mm^2
- Effective modular ratio $(\alpha_e) = \frac{E_s}{E_{c,eff}} = \frac{200}{25.45} = 7.86$

4.1.2.1 UNCRACKED TRANSFORMED SECTION

In the same method as in section 3.4.4.1, neutral axis depth and second moment of inertia are calculated as follows:

$\bar{y} = 155.51\ mm$

$I_{un} = 658642020.4\ \mathrm{mm}^4$

4.1.2.2 CRACKED TRANSFORMED SECTION

In the same method as in section 3.4.4.1, neutral axis depth and second moment of inertia of the fully cracked section are calculated as follows:

$x = 93.79\ \ mm$

$I_{cr} = 271618924.2\ \mathrm{mm}^4$

4.1.2.3 FLEXURAL CRACKING MOMENT

$f_r = 0.63\sqrt{f_c\ [Mpa]} = 0.63\sqrt{31.98[Mpa]} = 3.115\ Mpa$

y_t = h-x = 300-155.51 = 144.49 mm

$$\mathrm{M_{cr}} = \frac{f_\mathrm{r}\mathrm{I_{un}}}{\mathrm{y_t}} = \frac{3.115 * 658642020.4}{144.49} = 14.2\ \mathrm{kNm}$$

The section has cracked, since $M_{cr} < M$

4.1.2.4 SHORT TERM DEFELECTION

- For 20 kN load

$$Mid - span\ bending\ moment\ (M) = \frac{20\ x\ 1.8}{4} = 9\ kNm$$

:- The section has not cracked, since $M_{cr} < M$

Since the section is not cracked, the deflections may be calculated by using the elastic deflection equation as follows:

$$\delta = -\frac{PL^3}{48E_cI_e} = -\frac{20 * 1800^3}{48 * 25450 * 658642020.4} = -0.145\ mm$$

- For 50 kN load

$$Mid - span\ bending\ moment\ (M) = \frac{50\ x\ 1.8}{4} = 22.5\ kNm$$

:- The section has cracked, since $M_{cr} > M$

The effective second moment of the area is calculated by Eq. 2.11

$$I = \left(\frac{M_{cr}}{M}\right)^3 I_g + \left[1 - \left(\frac{M_{cr}}{M}\right)^3\right] I_{cr}$$
$$= \left(\frac{14.2}{22.5}\right)^3 658642020.4 + \left[1 - \left(\frac{14.2}{22.5}\right)^3\right] 271618924.2$$
$$= 368902998.08\ mm^4$$

Having calculated the effective moment of inertia, the deflections may be calculated by using the elastic deflection equation as follows:

$$\delta = -\frac{PL^3}{48E_cI_e} = -\frac{50 * 1800^3}{48 * 25450 * 368902998.08} = -0.647\ mm$$

- For 250 kN load

$$Mid - span\ bending\ moment\ (M) = \frac{250\ x\ 1.8}{4} = 112.5\ kNm$$

: - The section has cracked, since $M_{cr} > M$

The effective second moment of the area is calculated by Eq. 2.11

$$I = \left(\frac{M_{cr}}{M}\right)^3 I_g + \left[1 - \left(\frac{M_{cr}}{M}\right)^3\right] I_{cr}$$
$$= \left(\frac{14.2}{112.5}\right)^3 658642020.4 + \left[1 - \left(\frac{14.2}{112.5}\right)^3\right] 271618924.2$$
$$= 272397196.79\ mm^4$$

Having calculated the effective moment of inertia, the deflections may be calculated by using the elastic deflection equation as follows:

$$\delta = -\frac{PL^3}{48E_cI_e} = -\frac{250 * 1800^3}{48 * 25450 * 272397196.79} = -4.382\ mm$$

4.1.3 Calculation of Short Term Deflection in Accordance to ACI-318 with EC2 Material Property

The same procedure is taken as in section 4.1.1 with the material property taken from EC2. This is done to check whether the difference in the two codes approach is in the method or the material property.

- For 20 kN load

The uncracked second moment of the area is used since $M_{cr} > M$

$$\delta = -\frac{PL^3}{48E_cI_e} = -\frac{20 * 1800^3}{48 * 32470 * 225741879.52} = -0.118\ mm$$

- For 50 kN load

The effective second moment of the area is calculated by Eq. 2.11

$$I = \left(\frac{M_{cr}}{M}\right)^3 I_g + \left[1 - \left(\frac{M_{cr}}{M}\right)^3\right] I_{cr} = 267050783.49\ mm^4$$

Having calculated the effective moment of inertia, the deflections may be calculated by using the elastic deflection equation as follows:

$$\delta = -\frac{PL^3}{48E_cI_e} = -\frac{50 * 1800^3}{48 * 32470 * 267050783.49} = -0.701\ mm$$

- For 250 kN load

The effective second moment of the area is calculated by Eq. 2.11

$$I = \left(\frac{M_{cr}}{M}\right)^3 I_g + \left[1 - \left(\frac{M_{cr}}{M}\right)^3\right] I_{cr} = 226072350.75\ mm^4$$

Having calculated the effective moment of inertia, the deflections may be calculated by using the elastic deflection equation as follows:

$$\delta = -\frac{PL^3}{48E_cI_e} = -\frac{250 * 1800^3}{48 * 32470 * 226072350.75} = -4.138\ mm$$

4.1.4 Calculation of Short Term Deflection in Accordance to Bischoff's Method

The same procedure is taken as in the ACI-318 but the effective moment of inertia is calculated in equation shown below.

$$\frac{1}{I_e} = \left(\frac{M_{cr}}{M_a}\right)^m \frac{1}{I_g} + \left[1 - \left(\frac{M_{cr}}{M_a}\right)^m\right] \frac{1}{I_{cr}} \leq I_g$$

Therefore, taking the same data as in section 4.1.3, the deflection along the beam span is computed and presented as follows.

- For 20 kN load

$$\delta = -\frac{PL^3}{48E_cI_e} = -\frac{20 * 1800^3}{48 * 32470 * 635254929.23} = -0.118\ mm$$

- For 50 kN load

$$\delta = -\frac{PL^3}{48E_cI_e} = -\frac{50 * 1800^3}{48 * 32470 * 263007532.77} = -0.771\ mm$$

- For 250 kN load

$$\delta = -\frac{PL^3}{48E_cI_e} = -\frac{20 * 1800^3}{48 * 32470 * 226008673.76} = -4.139\ mm$$

4.1.5 Calculation of Short-term deflection Introducing Tension Stiffening

4.1.5.1 Stress vs. Strain diagram

The stress vs. strain diagram of the beam is calculated by using the code provides in Appendix A.

$$C_d = 7.5\ \times Diameter\ of\ the\ bar = 7.5 \times 20 = 150\ mm$$

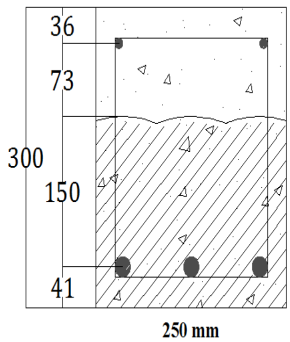

Figure 4-2: Proposed effective reinforced concrete section in the tension zone

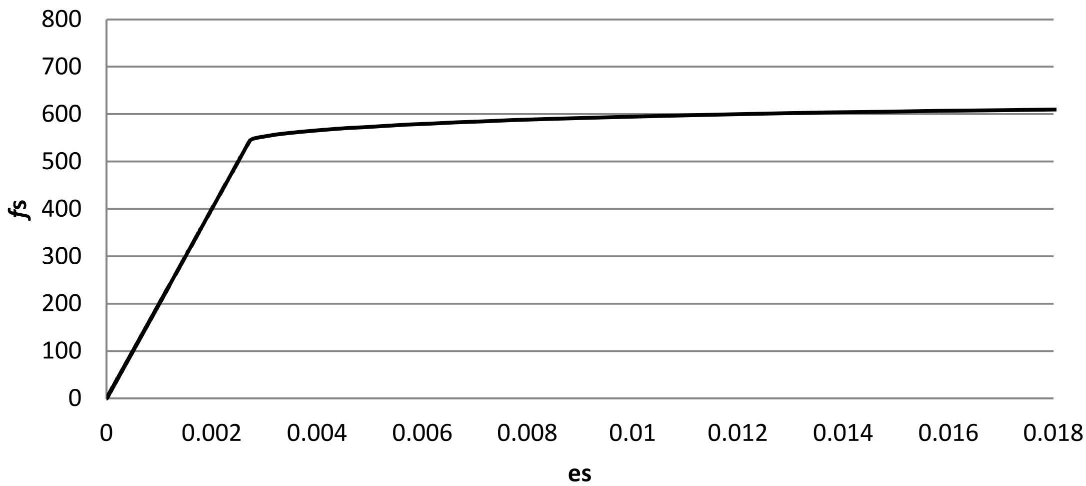

Figure 4-3: Stress vs. strain diagram proposed effective reinforced concrete section in the tension zone

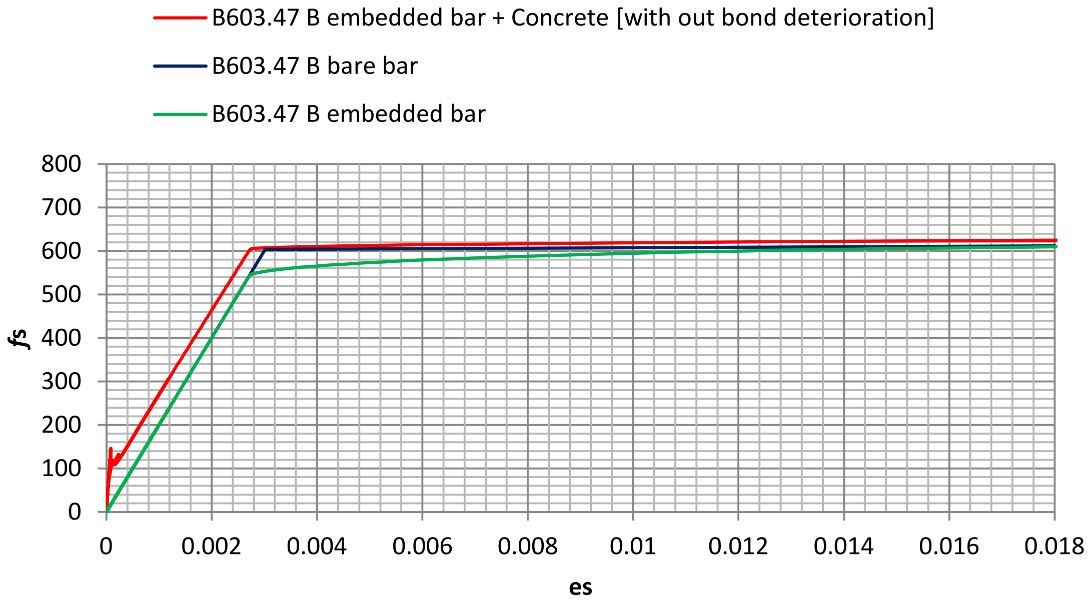

Figure 4-4: Comparison of the three stress vs. strain diagram in tension for the proposed effective concrete section in the tension zone

4.1.5.2 Calculation of Curvatures

Only the curvature of flexibility is calculated. Shrinkage and creep effect is ignored. In order to calculate the curvatures, the properties of the uncracked and cracked sections must first be calculated and the moment at which cracking occurs must be determined.

- For the concrete strength of 31.98 N/mm, E_{cm}=32472 N/mm^2
- For fully cracked section steel strength of 603.47 N/mm, Es=383.55 kN/mm^2
- Effective modular ratio $(\alpha_e) = \frac{E_s}{E_{c,eff}} = \frac{38\ 3.55}{32.47\ 2} = 12.3$

4.1.5.3 UNCRACKED TRANSFORMED SECTION

In the same method as in section 3.4.4.1, neutral axis depth and second moment of inertia are calculated as follows:

$\bar{y} = 158.52\ mm$

$I_{un} = 718619598.2\ \mathrm{mm}^4$

4.1.5.4 CRACKED TRANSFORMED SECTION

In the same method as in section 3.4.4.1, neutral axis depth and second moment of inertia of the fully cracked section are calculated as follows:

$x = 108.91\ mm$

$I_{cr} = 377327409.3\ \mathrm{mm}^4$

4.1.5.5 FLEXURAL CRACKING MOMENT

$$M_{cr} = \frac{f_{ctm} I_{un}}{y_t}$$

Where: f_{ctm} =2.67 N/mm

y_t = h-x = 300-158.52 = 141.48 mm

$$M_{cr} = \frac{f_{ctm} I_{un}}{y_t} = \frac{2.67 * 718619598.2}{141.48} = 13.41 \text{ kNm}$$

4.1.5.6 CALCULATION OF DEFLECTION

- For 20 kN load

$$Mid - span\ bending\ moment\ (M) = \frac{20\ x\ 1.8}{4} = 9\ kNm$$

:- The section has not cracked, since $M_{cr} > M$

$$\delta = -\frac{PL^3}{48E_cI_e} = -\frac{20 * 1800^3}{48 * 32472 * 718619598.2} = -0.105\ mm$$

- For 50 kN load

$$Mid - span\ bending\ moment\ (M) = \frac{50\ x\ 1.8}{4} = 22.5\ kNm$$

:- the section has cracked, since $M_{cr} < M$

In the same method as in section 3.4.4.6, Curvature and deflection are calculated and summarized by table as follows:

Table 4-4: Deflection Calculation of the above beam considering Tension stiffening

X/L	M. [kN/m]	X [mm]	ε [10^{-4}]	1/r [*10^{-6} rad/mm]	1St integral [10^3 rad]	2nd integral [10^3 mm]	Correction	Deflection [mm]
0.00	0.00	158.205	0.00	0.000	0.000	0.000	0.000	0.000
0.05	2.25	158.205	-	0.097	0.004	0.000	0.036	-0.036
0.10	4.50	158.205	-	0.195	0.018	0.001	0.072	-0.071
0.20	9.00	158.205	-	0.389	0.070	0.009	0.145	-0.136
0.30	13.50	156.806	0.428	0.428	0.144	0.028	0.217	-0.189
0.40	18.00	157.053	0.571	0.572	0.234	0.062	0.289	-0.227
0.50	22.50	112.109	1. 88	1.296	0.402	0.119	0.361	**-0.242**
0.60	18.00	157.053	0.571	0.572	0.570	0.207	0.434	-0.227
0.70	13.50	156.806	0.428	0.428	0.660	0.317	0.506	-0.189
0.80	9.00	158.205	-	0.389	0.733	0.443	0.578	-0.136
0.90	4.50	158.205	-	0.195	0.786	0.579	0.651	-0.071

0.95	2.25	158.205	-	0.097	0.799	0.651	0.687	-0.036
1.00	0.00	158.205	0.00	0.000	0.803	0.723	0.723	0.000

- For 250 kN load

$$Mid - span\ bending\ moment\ (M) = \frac{250\ x\ 1.8}{4} = 112.5\ kNm$$

:- the section has cracked, since $M_{cr} < M$

In the same method as in section 3.4.4.6, Curvature and deflection are calculated and summarized by table as follows:

Table 4-5: Deflection Calculation of the above beam considering Tension stiffening

X/L	M. [kN/m]	X [mm]	ε [10^{-4}]	1/r [*10^{-6} rad/mm]	1St integral [10^3 rad]	2nd integral [10^3 mm]	Correction	Deflection [mm]
0.00	0.00	158.205	0.00	0.000	0.000	0.000	0.000	0.000
0.05	11.25	158.205	-	0.487	0.022	0.001	0.493	-0.492
0.10	22.50	112.109	1.88	1.296	0.102	0.007	0.985	-0.979
0.20	45.00	87.875	7.23	4.273	0.603	0.070	1.971	-1.901
0.30	67.50	84.641	12.7	7.340	1.648	0.273	2.956	-2.683
0.40	90.00	84.732	18.2	10.574	3.261	0.715	3.941	-3.227
0.50	112.50	86.680	23.9	14.017	5.474	1.501	4.926	**-3.426**
0.60	90.00	84.732	18.2	10.574	7.687	2.685	5.912	-3.227
0.70	67.50	84.641	12.7	7.340	9.299	4.214	6.897	-2.683
0.80	45.00	87.875	7.23	4.273	10.344	5.982	7.882	-1.901
0.90	22.50	112.109	1.88	1.296	10.845	7.889	8.868	-0.979
0.95	11.25	158.205	-	0.487	10.926	8.868	9.360	-0.492
1.00	0.00	158.205	0.00	0.000	0.000	0.000	0.000	0.000

4.1.6 Calculation of Short-term Deflection By Introducing Bond Deterioration Zone on Tension Stiffening

4.1.6.1 Stress vs. Strain diagram

The stress vs. strain diagram of the beam is calculated by using the code provides in Appendix B.

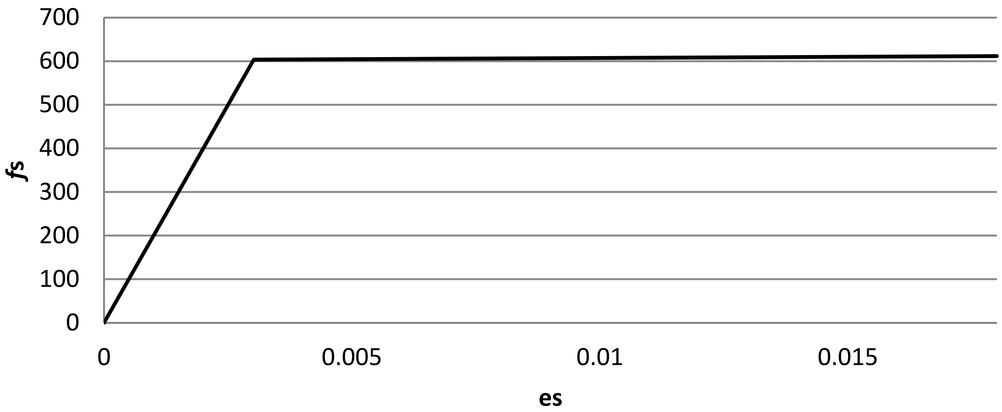

Figure 4-5: Stress vs. strain diagram proposed effective reinforced concrete section in the tension zone designated as proposed approach max.

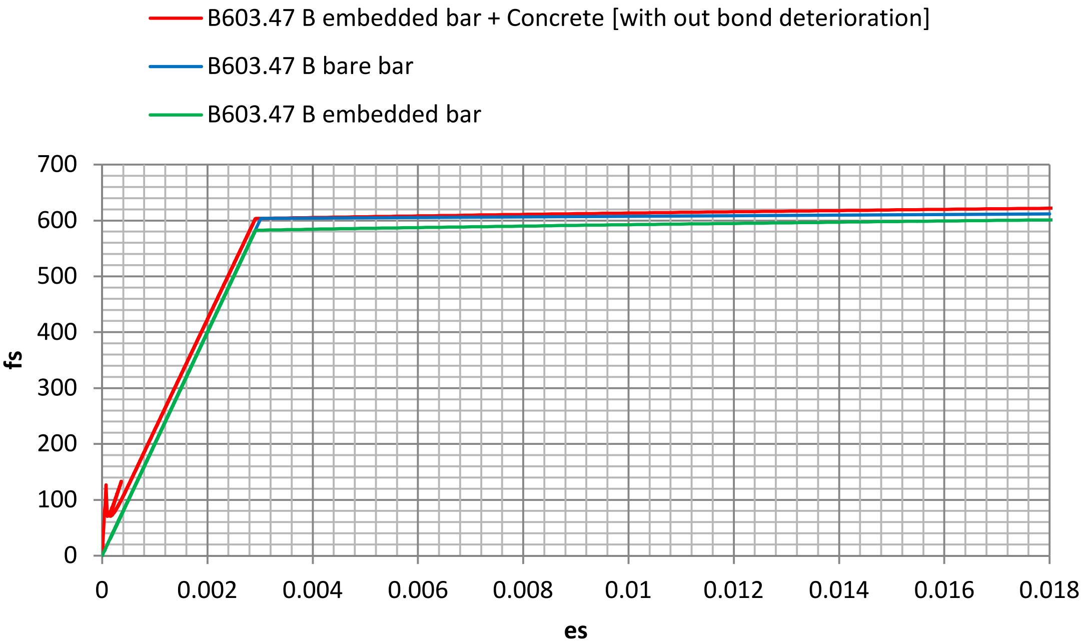

Figure 4-6: Comparison of the three stress vs. strain diagram in tension for the proposed effective concrete section in the tension zone designated as proposed approach max.

4.1.6.2 Calculation of Curvatures

Only the curvature of flexibility is calculated. Shrinkage and creep effect is ignored. In order to calculate the curvatures, the properties of the uncracked and cracked sections must first be calculated and the moment at which cracking occurs must be determined.

- For the concrete strength of 31.98 N/mm, E_{cm}=32472 N/mm^2
- For fully cracked section steel strength of 603.47 N/mm, Es=237.05 kN/mm^2
- Effective modular ratio $(\alpha_e) = \frac{E_s}{E_{c,eff}} = \frac{237.05}{32.47\ \ 2} = 7.3$

4.1.6.3 UNCRACKED TRANSFORMED SECTION

In the same method as in section 3.4.4.1, neutral axis depth and second moment of inertia are calculated as follows:

$\bar{y} = 155.108\ mm$

$I_{un} = 650978539.4\ \text{mm}^4$

4.1.6.4 CRACKED TRANSFORMED SECTION

In the same method as in section 3.4.4.1, neutral axis depth and second moment of inertia of the fully cracked section are calculated as follows:

$x = 91.38\ \ mm$

$I_{cr} = 256945717.3\ \text{mm}^4$

4.1.6.5 FLEXURAL CRACKING MOMENT

$$\text{M}_{\text{cr}} = \frac{f_{\text{ctm}}\text{I}_{\text{un}}}{\text{y}_{\text{t}}}$$

Where: f_{ctm} =2.67 N/mm

y_t = h-x = 300-155.11 = 144.89 mm

$$\text{M}_{\text{cr}} = \frac{f_{\text{ctm}}\text{I}_{\text{un}}}{\text{y}_{\text{t}}} = \frac{2.67 * 650978539.4}{144.89} = 11.99\ \text{kNm}$$

4.1.6.6 CALCULATION OF DEFLECTION

- For 20 kN load

$$Mid - span\ bending\ moment\ (M) = \frac{20\ x\ 1.8}{4} = 9\ kNm$$

:- The section has not cracked, since $M_{cr} > M$

$$\delta = -\frac{PL^3}{48E_cI_e} = -\frac{20 * 1800^3}{48 * 32472 * 650978539.4} = -0.115\ mm$$

- For 50 kN load

$$Mid - span\ bending\ moment\ (M) = \frac{50\ x\ 1.8}{4} = 22.5\ kNm$$

:- the section has cracked, since $M_{cr} < M$

In the same method as in section 3.4.4.6, Curvature and deflection are calculated and summarized by table as follows:

Table 4-6: Deflection Calculation of the above beam considering Tension stiffening

X/L	M. [kN/m]	X [mm]	ε [10-4]	1/r [*10-6 rad/mm]	1St integral [10³ rad]	2nd integral [10³ mm]	Correction	Deflection [mm]
0.00	0.00	155.108	0.00	0.000	0.00	0.0	0.0	0.000
0.05	2.25	155.108	-	0.106	0.00	0.0	0.1	-0.056
0.10	4.50	155.108	-	0.213	0.02	0.0	0.1	-0.111
0.20	9.00	155.108	-	0.426	0.08	0.0	0.2	-0.215
0.30	13.50	156.808	0.428	0.428	0.15	0.0	0.3	-0.307
0.40	18.00	100.368	1.97	1.259	0.31	0.1	0.4	-0.378
0.50	22.50	82.472	4.00	2.292	0.62	0.2	0.6	**-0.407**
0.60	18.00	100.368	1.97	1.259	0.94	0.3	0.7	-0.378
0.70	13.50	156.808	0.428	0.428	1.10	0.5	0.8	-0.307
0.80	9.00	155.108	-	0.426	1.17	0.7	0.9	-0.215
0.90	4.50	155.108	-	0.213	1.23	0.9	1.0	-0.111
0.95	2.25	155.108	-	0.106	1.24	1.0	1.1	-0.056
1.00	0.00	155.108	0.00	0.000	1.25	1.1	1.1	0.000

- For 250 kN load

$$Mid - span\ bending\ moment\ (M) = \frac{250\ x\ 1.8}{4} = 112.5\ kNm$$

:- the section has cracked, since $M_{cr} < M$

In the same method as in section 3.4.4.6, Curvature and deflection are calculated and summarized by table as follows:

Table 4-7: Deflection Calculation of the above beam considering Tension stiffening

X/L	M. [kN/m]	X [mm]	ε [10-4]	1/r [*10-6 rad/mm]	1St integral [10³ rad]	2nd integral [10³ mm]	Correction	Deflection [mm]
0.00	0.00	155.108	0.00	0.000	0.00	0.0	0.0	0.000
0.05	11.25	155.108	-	0.532	0.02	0.0	0.8	-0.826
0.10	22.50	82.472	4.00	2.292	0.15	0.0	1.7	-1.646
0.20	45.00	79.076	9.35	5.256	0.83	0.1	3.3	-3.212
0.30	67.50	79.677	14.7	8.312	2.05	0.4	5.0	-4.608
0.40	90.00	159.596	22.6	23.226	4.89	1.0	6.6	-5.638
0.50	112.50	142.307	28.2	24.594	9.19	2.2	8.3	**-6.025**
0.60	90.00	159.596	22.6	23.226	13.50	4.3	9.9	-5.638
0.70	67.50	79.677	14.7	8.312	16.34	7.0	11.6	-4.608
0.80	45.00	79.076	9.35	5.256	17.56	10.0	13.2	-3.212
0.90	22.50	82.472	4.00	2.292	18.24	13.2	14.9	-1.646
0.95	11.25	155.108	-	0.532	18.36	14.9	15.7	-0.826
1.00	0.00	155.108	0.00	0.000	18.39	16.5	16.5	0.000

4.1.7 Comparison

From the results we can have the following table summarizing the deflection calculation carried out for the 1.8m long beam.

Table 4-8: Summary of deflection calculation of B2M

P	δ ACI [mm]	δ ACI with EC2 material property [mm]	Bischoff's Method [mm]	δ EC2 [mm]	δ proposed considering tension stiffening [mm]	δ proposed considering tension stiffening and Bond deterioration Zone [mm]	Experiment
0	0.000	0.000	0.000	0.000	0.000	0.000	0.000
20	0.145	0.118	0.118	0.117	0.108	0.118	0.144
50	0.647	0.701	0.593	0.586	0.260	0.408	0.397
100	1.682	1.620	1.560	1.495	0.888	1.244	1.279
150	2.602	2.470	2.450	2.358	1.749	2.106	2.427
200	3.496	3.306	3.295	3.205	2.558	3.785	3.972
250	4.382	4.138	4.105	4.041	3.426	6.024	6.228
R^2	0.973165	0.971161	0.972718	0.9757	0.991478	0.999177	

As the results imply the deflection is significantly small when calculated considering the role of concrete still intact between consecutive cracks. Whereas, considering the impact of the splitting and crushing of concrete around the bar next to the crack surface will give more reliable result. In a similar method other Beams are assessed.

4.2 Deflection Calculation of Specimen B1M

From the research Fatigue behavior of shear-critical reinforced concrete beams (Getachew, 2018), Specimen B1M is used. This beam is tested under a monotonically increasing load, 101 days after casting. From the experimental result the cube compression strength is 33.58 N/mm, tensile strength is 2 N/mm and steel yield strength of 603.47 N/mm. The cross section of the beam is shown in Figure 4-7.

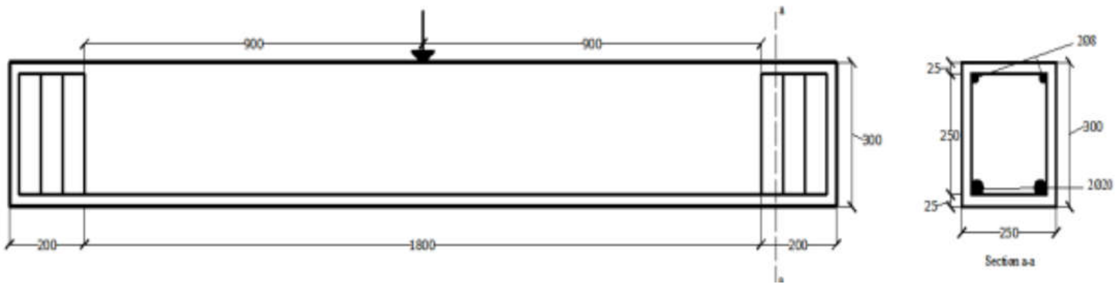

Figure 4-7: Specimen B1M (Getachew, 2018)

Similar method to section 4.1 is used for deflection calculation and to minimize replication it is summarize by table as follows:

Table 4-9: Summary of deflection calculation of B1M

P [kN]	**δ ACI [mm]**	**δ ACI with EC2 material property [mm]**	**Bischoff's Method [mm]**	**δ EC2 [mm]**	**δ proposed considering tension stiffening [mm]**	**δ proposed considering tension stiffening and Bond deterioration Zone [mm]**	**Experment**
0	0.000	0.000	0.000	0.000	0.000	0.000	0.000
50	1.893	1.998	2.599	1.980	0.702	1.455	1.476
100	3.491	3.596	4.197	3.578	2.300	3.053	3.074
160	5.408	5.513	6.114	5.495	4.217	4.970	4.991
R^2	0.998147	0.997208	0.989344	0.997379	0.990370	0.999994	

4.3 Deflection Calculation of Specimen MB

From ongoing research by Noah Girma for Investigation of shear fatigue in reinforced concrete bridge girder, Specimen MB is used. This beam is tested under a monotonically increasing load. From the experimental result the cube compression strength is 34.61 and steel yield strength of 617.12. The cross section of the beam is shown in Figure 4-8.

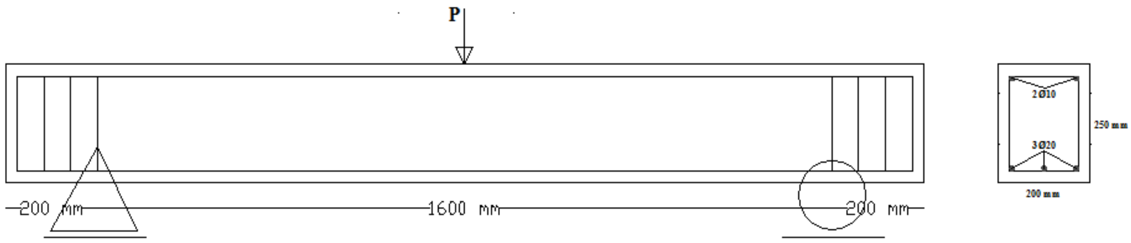

Figure 4-8: Specimen MB

Similar method to section 4.1 is used for deflection calculation and to minimize replication it is summarize by table as follows:

Table 4-10: Summary of deflection calculation MB

P [kN]	δ ACI [mm]	δ ACI with EC2 material property [mm]	Bischoff's Method [mm]	δ EC2 [mm]	δ proposed considering tension stiffening [mm]	δ proposed considering tension stiffening and Bond deterioration Zone [mm]	Experiment
0	0	0	0	0	0	0	0.000
15	0.158	0.0855	0.0886	0.128	0.125	0.115	0.054
35	0.487	0.444	0.451	0.424	0.359	0.226	0.214
50	0.975	0.974	0.987	0.861	0.7059	0.391	0.450
75	1.509	1.448	1.466	1.398	1.225	0.811	1.070
100	2.143	2.009	2.034	2.034	1.840	1.309	1.806
R^2	0.97908	0.97153	0.97147	0.98496	0.99121	0.998136	

4.4 Deflection Calculation of Specimen BC1

From the research Enhancement of the Flexural Behavior of CFRP Strengthened RC Beams in Medium and Low Grade Concrete (Negussie, 2018), Specimen BC1 is used. This beam is tested under a monotonically increasing load. From the experimental result the cube compression strength is 33.52 N/mm and steel yield strength of 545.37 N/mm. The cross section of the beam is shown in Figure 4-9.

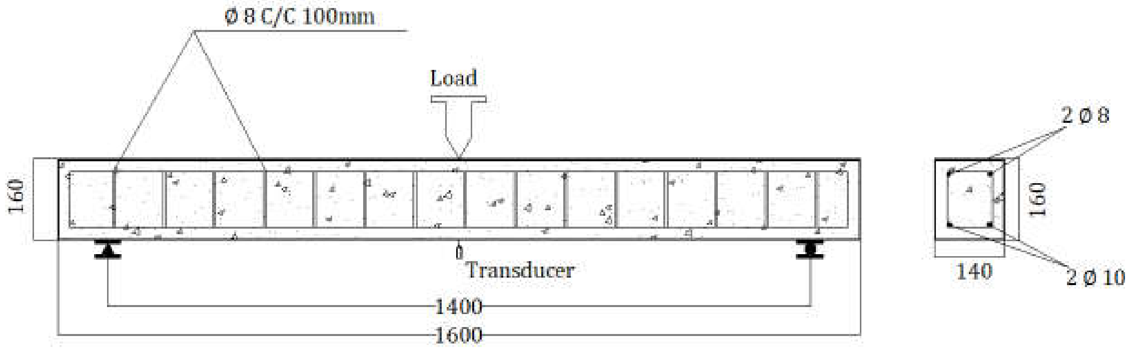

Figure 4-9: Specimen BC1 (Negussie, 2018)

Similar method to section 4.1 is used for deflection calculation and to minimize replication it is summarize by table as follows:

Table 4-11: Summary of deflection calculation BC1

P	δ ACI [mm]	δ ACI with EC2 material property [mm]	Bischoff's Method [mm]	δ EC2 [mm]	δ proposed considering tension stiffening [mm]	δ proposed considering tension stiffening and Bond deterioration Zone [mm]	Experiment
0	0.000	0.000	0.000	0.000	0.000	0.000	0.000
5	0.313	0.265	0.313	0.265	0.242	0.279	0.285
10	1.209	1.109	1.319	1.100	0.735	1.043	1.048
15	2.787	2.597	3.089	2.571	1.605	2.389	2.392
20	4.829	4.541	5.068	4.398	3.329	3.996	4.039
25	6.870	6.484	7.045	6.225	5.052	5.603	5.684
R^2	0.999895	0.999809	0.999804	0.999962	0.994636	0.999983	

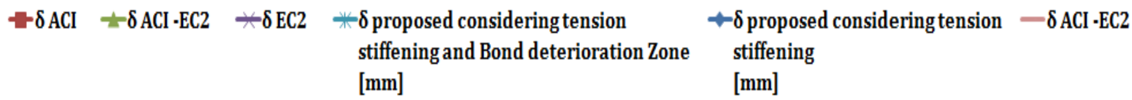

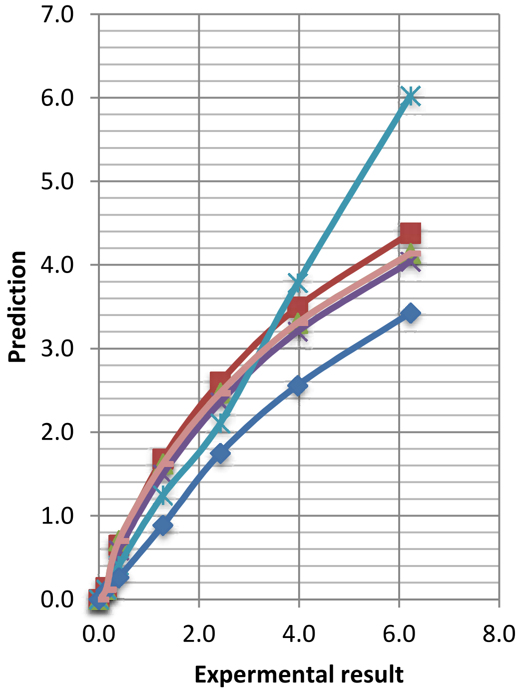

Figure 4-10: Prediction vs. Experimental Deflection Chart of B2M

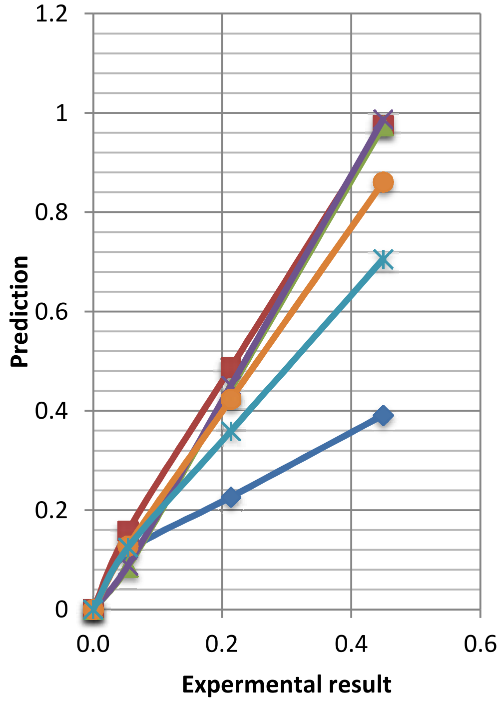

Figure 4-12: Prediction vs. Experimental Deflection Chart of MB

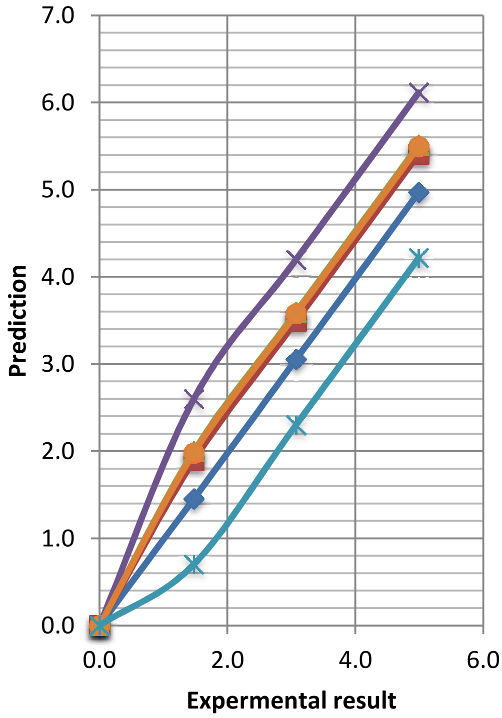

Figure 4-11: Prediction vs. Experimental Deflection Chart of B1M

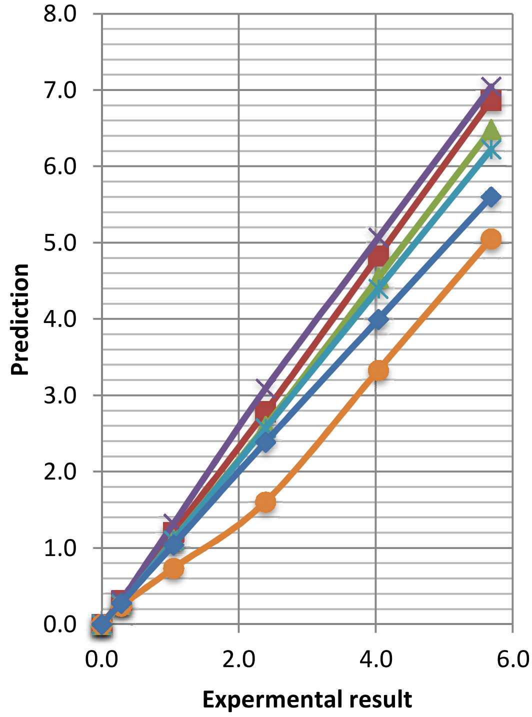

Figure 4-13: Prediction vs. Experimental Deflection Chart of BC1

These charts show experimental result vs. predicted values. From the depicted charts we clearly understood that the code predicted values are not linear. In addition, these predicted values give a lower value than the experimental result. The result that is obtained by considering tension stiffening gives a very high result. The reason for the higher result is that the bond deterioration zone is not included in the analysis. The proposed method which include bond deterioration zone on tension stiffening gives a linear result. The result is closer to the experimental result.

5. CONCLUSION AND RECOMMENDATION

5.1 Conclusion

In this thesis, the influence of bond deterioration zone on tension stiffening of flexural members on short-term deflection has been observed. In numerical modeling, the rational, accurate and versatile consideration of the stress transfer ability of cracked RC elements is crucial in order to predict accurately the cracking response, strength, deflection and failure mode of RC structures.

The following conclusions are made on the basis of analytical investigation and experimental verification results.

- In reinforced concrete members with ordinary reinforcement ratios, tension softening at the crack surface can be neglected without significant influence on the average response of the concrete and reinforcement. However, in very lightly reinforced concrete or plain concrete, tension softening at fractured crack planes is predominant and has to be taken into consideration.
- Due to the composite nature of reinforced concrete deflection of reinforced concrete flexural members is more of a member property rather than a section. Design codes and methods discussed address deflection as a function of a section that behaves in a state between totally intact or totally cracked, depending on its state of stress. But these approaches fail to fully incorporate the tension stiffening effect which mainly is the attribute of the intact concrete between cracked sections and bond deterioration zone which is deterioration of bond due to splitting conical cracks.
- A method to consider tension stiffness and bond deterioration of a reinforced concrete element in deflection calculation is proposed. The average stress-strain relationship of embedded bar was formulated. The yielding point of the average stress-strain curve of the steel bar in reinforced concrete is lower than that of the bare bar and the modulus of elasticity of a bare bar is less than steel bar in reinforced concrete.

- Design codes (ACI Commitee 318, 2014; European Standard, 1992) gives over estimated deflection value. This is because even after crack propagates concrete between cracks carries tensile force. The proposed approach considering the role of concrete still intact between consecutive cracks gives underestimated deflection value. Whereas, considering the impact of the splitting and crushing of concrete around the bar next to the crack surface will give more reliable result.

5.2 Recommendation

The approach proposed is the analysis of the average stress-stress tensile relationship between cracked concrete and embedded reinforcement by direct theoretical derivation. This paper investigates an approach in calculating the immediate deflection of a reinforced concrete beam under the load. After examining these analyses, the following recommendations are put forward:

- The defined efficient concrete region in tension should be addressed for everyday design practice. Since in codes and standards the effective area of concrete in tension does not specify whether or not it is equally effective in tension stiffening and bond deterioration.
- This thesis focuses only on the role of bond deterioration zone in short term deflection of reinforced concrete. Parameters such as load variation, shear reinforcement confinement effect, reduction and other time-related variables, such as creep and concrete maturation, play a major role in the long term. Therefore, in future works, the author intends to address such issues.

APPENDIX A

```
!ADDIS ABABA UNIVERSITY
!Addis Ababa institute of Technology
!School of Civil and Environmental Engineering
!Bezawit Temesgen-GSR/1205/08
Program
Smeared_Stress_Strain_Curve_of_Mild_Steel_Embeded_in_Concrete
_considering _Tenshion_Stiffening
implicit none
! Variables are declared.
real:: esxi(100),esx_,ecr,ch_es,esi,exi,esi_                !!! strain
real:: fyd,C,fck,Ec,fcr,Ac,fc(100),fbr,fci                    !!!
Concrete property
real:: fyk,As                                      !!! Steel property

real:: fsx(100),fsx_,fss,fsxi(100),fxi             !!! smeared stress
strain
real:: ro,L,ch_x,s(100),n,Taw,d,S_,Taw_   ! s(70) & S_ are slip, ro is
reinforcement ratio, L & d is length and diameter, n is no of crack,
Taw & Taw_ are bond stress
real,Parameter:: pi=3.1415927,eul=2.718281828459,k=0.73,c_=3,E_s=200000
integer::i,j,p
! Data entry
Print*, "please enter the following material properties and cross
sectional parameters"
Print*, "the class of concrete in use(limited from C15 to C60). e.g for
C25 input 25"
Read*,C
fck=C
fcr=max(0.31*sqrt(fck),2.6)
Ec=max(9500*((fck+8)**(1.0/3.0)),31000)
ecr=fcr/E_s
Print*, "summary of the concrete property used"
Print*, "fck=",fck,"Mpa"
Print*, "fcr=",fcr,"Mpa"
Print*, "Ec=",Ec,"Mpa"
Print*, "ecr=",ecr,"mm/mm"
Print*, "_____________________________________________________________"
Print*, "the grade of reinforcing bar used. e.g. for S300 input 300"
Read*,fyk
fyd=fyk
Print*, "summary of the reinforcing bar property used"
Print*, "fyk=",fyk,"Mpa"
Print*, "fyd=",fyd,"Mpa"
Print*, "Es=",E_s,"Mpa"
Print*, "_____________________________________________________________"
Print*, "area of reinforcement in tension zone in mm2"
Read*,As
```

```
Print*, "diameter of reinforcement in tension zone in mm"
Read*,d
Print*, "area of concrete in tension zone in mm2"
Read*,Ac
ro= As/Ac
Print*, "reinforcement ratio is",ro
Print*, "___________________________________________________________"
Print*, "Please enter center to center length of the beam in mm"
Read*,L
print*,"strain             steel Stress   Concrete Stress"
n=0
do esi_=0,0.15,0.00001
ch_x=((L/(1+n))/2)/100
S_=0
Taw_=0
esx_=esi_
esi=esi_
  Do j=1,100,1
         ch_es=0
             Do i=1,10,1
                IF(esi<(fyd/E_s))then
                    fss=esi*E_s
                Else
                    fss=fyd
                End if
   fsx_=fss
   S(j)=S_+(ch_x*(2*esi+ch_es)/2)

Taw=(fck*k*log(1+5*(1000*S(j)/d))**c_)*(1/(1+(100000*(esi+ch_es))))
    fsx(j)=fsx_+(pi*d*ch_x*(((Taw_+Taw)/2)/As))

        IF(fsx(j)<fyd)then
           ch_es=(fsx(j)/E_s)-esi
        Else
           ch_es=(fyd/E_s)-esi
        End if
           End do
esi=esi+ch_es
fsxi(j)=(fsx_+fsx(j))*ch_x/2
esxi(j)=(esx_+esi)*ch_x/2
S_=S(j)
Taw_=Taw
fsx_=fsx(j)
esx_=esi
End do
       fxi=sum(fsxi)/((L/(1+n))/2)
       exi=sum(esxi)/((L/(1+n))/2)
!! calculate bridging stress (Tenshion softnening)
fbr=fcr*(1+(0.5*(fcr/0.15)*(2/1.3)*maxs(s)))**(-3)
!! calculate concrete tensile strength
```

```
fci=ro*(maxf(fsx)-fxi)+fbr
      do p=1,100,1
         fc(p)=ro*(maxf(fsx)-fsx(p))+fbr
      end do
print*,exi,fxi,fci
         !! calculate the no of crack
              IF(maxc(fc)>fcr)then
                 n=n+1
              End if
    !output data to a file
    OPEN( unit=10, FILE = 'D:\result_without_bond_deterioratin_zone
.txt', position='append')
    WRITE (10,*) exi,fxi,fci
    CLOSE (10)
End do
    !!! a function to find the maximum value of sleep
Contains
function maxs(s)
   real:: s(100),maxs
   maxs=s(1)
    do i=2,100,1
      if(s(i)>maxs)then
          maxs=s(i)
      end if
    end do
end function
    !!! a functon to find the maximum value of embedded steel stress
function maxf(fsx)
   real:: fsx(100),maxf
   maxf=fsx(1)
    do i=2,100,1
      if(fsx(i)>maxf)then
          maxf=fsx(i)
      end if
    end do
end function
    !!! a functon to find the maximum value of Concrete stress
function maxc(fc)
   real:: fc(100),maxc
   maxc=fc(1)
    do i=2,100,1
      if(fc(i)>maxc)then
          maxc=fc(i)
      end if
    end do
end function
end program
Smeared_Stress_Strain_Curve_of_Mild_Steel_Embeded_in_Concrete_consideri
ng_Tenshion_Stiffening
```

APPENDIX B

```
!ADDIS ABABA UNIVERSITY
!Addis Ababa institute of Technology
!School of Civil and Environmental Engineering
!Bezawit Temesgen-GSR/1205/08
Program Smeared_Stress_Strain_Curve_of_Mild_Steel_Embeded_in_Concrete
_considering_bond_deterioration_zone
implicit none
! Variables are declared.
real:: esxi(100),esx_,ecr,ch_es,esi,exi,esi_    !!! strain
real:: fyd,C,fck,Ec,fcr,Ac,fc,fbr,fci           !!! Concrete property
real:: fyk,As                                   !!! Steel property
real:: fsx(70),fsx_,fss,fsxi(70),fxi      !!smeared stress strain
real:: ro,L,ch_x,s(70),n,Taw(70),d,S_,Taw_,lb         ! s(70) & S_ are
slip, ro is rainforsement ratio, L & d is length and diameter, n is
no of crack, Taw & Taw_ are bond stress,lb is deteriorated length
real,Parameter:: pi=3.1415927,eul=2.718281828459,k=0.73,c_=3,E_s=200000
integer::i,j

! Data entry
Print*, "please enter the following material properties and cross
sectional parameters"
Print*, "the class of concrete in use(limited from C15 to C60). e.g for
C25 input 25"
Read*,C
fck=C
fcr=max(0.31*sqrt(fck),2.6)
Ec=max(9500*((fck+8)**(1.0/3.0)),31000)
ecr=fcr/E_s
Print*, "summary of the concrete property used"
Print*, "fck=",fck,"Mpa"
Print*, "fcr=",fcr,"Mpa"
Print*, " Ec=",Ec,"Mpa"
Print*, "ecr=",ecr,"mm/mm"
Print*, "___________________________________________________________"
Print*, "the grade of reinforcing bar used. e.g. for S300 input 300"
Read*,fyk
fyd=fyk
Print*, "summary of the reinforcing bar property used"
Print*, "fyk=",fyk,"Mpa"
Print*, "fyd=",fyd,"Mpa"
Print*, " Es=",E_s,"Mpa"
Print*, "___________________________________________________________"
Print*, "area of reinforcement in tension zone in mm2"
Read*,As
Print*, "diameter of reinforcement in tension zone in mm"
Read*,d
Print*, "area of concrete in tension zone in mm2"
Read*,Ac
```

```
ro= As/Ac
Print*, "reinforcement ratio is",ro
Print*, "____________________________________________________________"
Print*, "Please enter center to center lenth of the beam in mm"
Print*, L
lb=10*d
Print*, "   strain            steel Stress            Concrete Stress"
n=0
do esi_=0,0.15,0.00001
      esi=esi_
      S_=0
      Taw_=0
      esx_=esi_
      ch_x=(((L/(1+n))/2)-lb)/50
            Do j=1,70,1
if(j<=50)then
      ch_es=0
      Do i=1,10,1
      IF(esi<=(fyd/E_s))then
            fss=esi*E_s
      Else
            fss=fyd
      End if
          fsx_=fss
          S(j)=S_+(ch_x*(2*esi+ch_es)/2)
Taw(j)=(fck*k*log(1+5*(1000*S(j)/d))**c_)*(1/(1+(100000*(esi+ch_es))))
          fsx(j)=fsx_+(pi*d*ch_x*(((Taw_+Taw(j))/2)/As))
      IF(fsx(j)<=fyd)then
         ch_es=(fsx(j)/E_s)-esi
      Else
          ch_es=(fyd/E_s)-esi
      End if
      End do                  !for Do @ line 61
 esi=esi+ch_es
 S_=S(j)
 Taw_=Taw(j)
 fsxi(j)=(fsx_+fsx(j))*ch_x/2
 esxi(j)=(esx_+esi)*ch_x/2
 fsx_=fsx(j)
 esx_=esi
Else  !for if @ line 59
ch_x=Lb/20
If((((j-50)*ch_x)+((L/2)-lb))<=((L/2)-(lb/2)))then
Taw(j)=Taw(50)-(Taw(50)/lb)*((((j-50)*ch_x)+((L/2)-lb))-((L/2)-lb))
Else
Taw(j)=0
End If
fsx(j)=fsx_+(pi*d*ch_x*(((Taw_+Taw(j))/2)/As))
      IF(fsx(j)<=fyd)then
       esi=fsx(j)/E_s
      Else
       esi=fyd/E_s
      End if
```

```
S(j)=S(j-1)+(ch_x*(esi+esx_)/2)
ch_es=0
fsxi(j)=(fsx_+fsx(j))*ch_x/2
esxi(j)=(esx_+esi)*ch_x/2
Taw_=Taw(j)
fsx_=fsx(j)
esx_=esi
End if   !for if @ line 59
End do   !for Do @ line 58
       fxi=sum(fsxi)/(((L/(1+n))/2))
       exi=sum(esxi)/(((L/(1+n))/2))
!! calculate bridging stress (Tenshion softnening)
fbr=fcr*(1+(0.5*(fcr/0.15)*(2/1.3)*maxs(s)))**(-3)
!! calculate concrete tensile strength
fci=ro*(maxf(fsx)-fxi)+fbr
fc=ro*(maxf(fsx)-minf(fsx))+fbr
print*,exi,fxi,fci
!output data to a file
OPEN( unit=10, FILE =
'D:\result_considering_bond_deterioration.txt',position='append')
WRITE (10,*)exi,fxi,fci
CLOSE (10)
!! calculate the no of crack
IF(fc>fcr)then
n=n+1
End if
end do ! for do @ line 52
!!! a functon to find the maximum value of sleep
Contains
function maxs(s)
   real:: s(70),maxs
   maxs=s(1)
    do i=2,70,1
      if(s(i)>maxs)then
          maxs=s(i)
      end if
    end do
end function
!!! a functon to find the maximum value of embedded steel stress
function maxf(fsx)
   real:: fsx(70),maxf
   maxf=fsx(1)
    do i=2,70,1
      if(fsx(i)>maxf)then
          maxf=fsx(i)
      end if
    end do
end function
!!! a functon to find the minimum value of embedded steel stress
function minf(fsx)
   real:: fsx(70),minf
   minf=fsx(1)
    do i=2,70,1
```

```
      if(fsx(i)<minf)then
          minf=fsx(i)
      end if
    end do
end function
end program Smeared_Stress_Strain_Curve_of_Mild_Steel_Embeded_in_
Concrete_considering_bond_deterioration_zone
```

REFERENCES

ACI 318. (2008). Building Code Requirements for structural concrete. *American Concrete Institute Committee 318* .

ACI Commitee 318. (2014). *Building Code Requirements for Structural Concrete (ACI 318-14) AND Commentary on Building Code Requirements for Structural Concrete (ACI 318R-14).* American Concrete Institure.

Belarbi, A., & Hsu, T. (1991). Constitutive laws of RC in biaxial tension-compression.

CEP-FIP. (1978). *Model Code for C0ncrete Structures: CEP-FIP International Recommendations Model Code 1990.* Parus: Comite EuroInternational du Beton.

EBCS 2. (1995). Ethiopian Building Code Standard. *Structural Use of Concrete"* .

EC 2. (1992). Eurocode 2 - Design of Concrete Structures - Part 1. *Eurocode EC 2* .

European Standard. (1992). *Eurocode 2: Design of Concrete Structures.* European Commitee for Standardization.

Getachew, T. (2018). *Fatigue behavior of shear-critical Reinforced Concrete beams.* Addis Ababa: ADDIS ABABA UNIVERSITY.

Goto, Y. (1971). Crack formed in concrete around deformed tenshion bars. *ACI Journal, V. 68* , 244-251.

Hsu, T. C., Thomas, & Mo, Y. L. (2010). *Unified Theory of Concrete Structures.* USA: University of Houston.

Maekawa K., & Qureshi J. (1996). Embedded bar behavior in concrete under combined axial pullout and transverse combined axial pullout and transverse displacement. pp. 183-195.

Maekawa, K., Pimanmas, A., & Okamura, H. (2004). *Nonlinear Mechanics of Reinforced Concrete.* London : Spon Press .

Mishima, T., Yamada, K., & Maekawa, K. (1992). Localized deformational behavior of a crack in RC plates subjected to reversed cyclic loads. pp. 161-170.

Negussie, A. (2018). *Enhancement of the Flexural Behavior of CFRP Strengthened RC Beams in Medium and Low Grade Concrete.* Addis Ababa : Addis Ababa University.

Qureshi, J., & Maekawa , K. (1996). Computational model for reinforcing bar embedded in concrete under combined axial pullout and transverse displacement. pp. 227-239.

Salem, H., & Maekawa, K. (1999). Spatially average tensile mechanics for cracked concrete and reinforcement under highly inelastic range. pp. 277-293.

Shima H. , Chou L. , & Okamura, H. . (1987). Micro and macro models for bond in reinforced concrete. *Journal of the faculty of Engineering , 39*.

Soltani, M., An, X., & Maekawa, K. (2003). Computational model for post cracking analysis of RC membrane elements based on local stress–strain characteristics. *Engineering Structures* , 993-1007.

Tadesse, y. (2015). Tension Property of Concrete and its Role in the Immediate Deflection of Reinforced Concrete Beams under Serviceability Limit State. Addis Ababa.